

UNIVERSITAT POLITÈCNICA DE VALÈNCIA

ESCOLA TÈCNICA SUPERIOR D'ENGINYERIA
AGRONÒMICA I DEL MEDI NATURAL



Characterization of the interaction between PP1 and Caspase 9 in apoptosis

Collaborates:



DEGREE FINAL PROJECT. BIOTECHNOLOGY

AUTHORESS:

Miriam Guillén Navarro

TUTOR:

María Adelaida Gimeno García

COTUTORS:

Jerónimo Bravo Sicilia

Leticia Domínguez Berrocal

Academic year: 2014-2015

VALENCIA, July 2015



A. SUMMARY

Characterization of the interaction between PP1 and caspase 9 in apoptosis

Apoptosis is a highly regulated form of programmed cell death that eliminates individual cells in a controlled way, playing a key role in the maintenance of tissue homeostasis. Apoptotic cell death is deregulated in some conditions, such as cancer, having devastating effects in the organism. The main executors in this process are a family of cysteine aspartatyl-specific proteases, caspases, which induce controlled cell death by cleaving target cellular proteins in specific aspartic residues. Caspase 9 is the last initiator caspase in the caspase-dependent apoptotic pathway and it is able to process and activate caspases 3,6 and 7, amplifying the apoptotic signal. From this point on, the execution of cell death is irreversible. Due to its function, caspase 9 represents a molecular target in cancer therapy strategies. Dessauge *et al* (2006) have demonstrated that PP1 α directly dephosphorylates caspase 9, activating it, thus promoting its protease activity and the irreversible cell entry in apoptosis. PP1 is an ubiquitous serine/threonine phosphatase that regulates different important cellular processes. It dephosphorylates hundreds of crucial biological targets and its apoenzyme is associated with more than 200 regulatory proteins to form specific holoenzymes. The characterization of the PP1-caspase 9 interaction would provide useful information about the molecular mechanism of caspase 9 activation in the context of apoptosis. For this purpose, the human proteins have been overexpressed as fusion proteins in BL21 or BL21 codon plus *E.coli* strains. Several constructs of PP1 and caspase 9 were purified by using both affinity chromatography and size-exclusion chromatography to perform further interaction assays. Binding characterization using pull-down assays and biophysical techniques such as Biolayer Interferometry (BLI) and Isothermal Titration Calorimetry (ITC) verified a weak interaction between PP1 and caspase 9 full length, but not with CARD or Δ CARD domains. This suggests that the strength of the interaction depends on several binding sites and it may occur before caspase 9 *in vivo* processing. Further strategies using caspase 9 phosphomimetic mutants designed in this work will provide more information about the residues involved in the affinity of the interaction.

Key words: PP1, caspase 9, phosphatase, apoptosis, purification, binding, BLI, ITC, pull-down

Author: Miriam Guillén Navarro Valencia, July 2015

Tutor: María Adelaida García Gimeno

Cotutors: Jerónimo Bravo Sicilia, Leticia Domínguez Berrocal

B. RESUMEN

Caracterización de la interacción entre caspasa 9 y PP1 en apoptosis

La apoptosis es una forma de muerte celular fuertemente regulada que elimina células de una manera controlada, jugando un papel crucial en el mantenimiento de la homeostasis de los tejidos. Existe un desequilibrio en el proceso de muerte celular en algunas patologías como el cáncer, lo que tiene efectos devastadores en el organismo. Los ejecutores principales de este proceso son una familia de cistein proteasas específicas de aspártico, las caspasas, que inducen la muerte celular controlada mediante el procesamiento proteolítico de otras proteínas diana de la célula. Caspasa 9 es la última de las caspasas iniciadores y es capaz de procesar y activar a las caspasas 3,6 y 7, amplificando la señal apoptótica. A partir de este punto, la señal de muerte celular es irreversible. Debido a su función, caspasa 9 representa una diana molecular para el desarrollo de terapias contra el cáncer. Dessauge et al. (2006) demostraron que PP1 α desfosforila a caspasa 9 de manera directa, activándola, y por ende promoviendo tanto su actividad como proteasa como la entrada de la célula en apoptosis. PP1 es una fosfatasa de serina/treonina ubicua que regula diferentes procesos celulares. Desfosforila cientos de dianas celulares y su apoenzima se asocia con más de 200 proteínas reguladoras para formar holoenzimas específicas. La caracterización de la interacción entre PP1 y caspasa 9 aportará información relevante en el mecanismo de activación de caspasa 9 en el contexto de apoptosis. Para ello, ambas proteínas se sobreexpresaron como proteínas de fusión en las cepas BL21 o BL21 codon plus de *E.coli*. Varias construcciones de PP1 y caspasa 9 fueron purificadas usando cromatografía de afinidad y cromatografía de exclusión molecular para llevar a cabo ensayos de interacción adicionales. La caracterización de la unión se realizó usando ensayos *pull-down* y técnicas biofísicas como interferometría de biocapa o calorimetría isoterma de titulación verificaron la existencia de una interacción débil entre PP1 y caspasa 9 completa, pero no con los dominios CARD y Δ CARD de caspasa 9. Esto sugiere que la fuerza de la unión reside en múltiples puntos de anclaje y que esta unión se produce antes de que caspasa 9 sea procesada *in vivo* en la célula. Se desarrollarán nuevas estrategias usando los mutantes fosfomiméticos diseñados en el presente trabajo, que proporcionarán más información sobre los residuos implicados en la unión.

Palabras clave: PP1, caspasa 9, fosfatasa, apoptosis, purificación, interacción, BLI, ITC, *pull-down*

Autora: Miriam Guillén Navarro Valencia, Julio 2015

Tutora: María Adelaida García Gimeno

Cotutores: Jerónimo Bravo Sicilia, Leticia Domínguez Berrocal

C. AGRADECIMIENTOS

En primer lugar, quiero destacar a las personas con las que he pasado más horas durante todo este año, mis compañeros de laboratorio. A Jero por darme la oportunidad de trabajar en su equipo. A Susana, por estar siempre dispuesta a ayudarme. A Angélica, Nada, Sara, Ana, Alejandro y Marcin, que no sólo me han ayudado siempre sino que me han hecho pasar grandes momentos tanto dentro como fuera del laboratorio. Y en especial a Leti, por convertirme en su “pequeño saltamontes”, por compartir tantos buenos ratos en no siempre buenos momentos y enseñarme tanto a cambio de tan poco. Realmente formamos un gran equipo y estoy segura de que nos volveremos a encontrar.

En segundo lugar, me gustaría nombrar a la persona que me dio mi primera oportunidad en esto de la ciencia, el cual ha creído siempre en mí y me ha dado un empujoncito cuando más lo necesitaba. Gracias Alex.

Agradecer a mis padres todo el apoyo recibido, no solo este año sino durante toda mi vida. Sin ellos, nada de esto sería posible. También a Eli mi compañera de ya tantas cosas, gracias por formar parte de este camino que hemos recorrido juntas y por enseñarme tantas cosas buenas.

Y por último, a la persona más especial. A Edgar por ser mi gran apoyo y acompañarme en todo momento, por su paciencia y por darme a diario la fuerza que necesito para alcanzar todos mis sueños.

*“Lo que sabemos es una gota de agua;
lo que ignoramos es el océano”*

Isaac Newton

INDEX

A. SUMMARY	I
B. RESUMEN	II
C. AGRADECIMIENTOS.....	III
1. INTRODUCTION	1
1.1. APOPTOSIS	1
1.2. CASPASES.....	1
1.2.1. Caspases and its role in apoptosis.....	1
1.2.2. Caspase 9.....	3
1.2.3. Regulation of caspases	4
1.3. PROTEIN PHOSPHATASE 1.....	5
1.4. PP1 - CASPASE 9 INTERACTION IN CASPASE-DEPENDENT APOPTOTIC PATHWAY	6
2. OBJECTIVES.....	7
3. MATERIALS AND METHODS	7
3.1. CASPASE 9	7
3.1.1. Cloning.....	7
3.1.2. Site-directed mutagenesis.....	9
3.1.3. Low-scale overexpression	10
3.1.4. Low-scale purification	11
3.1.5. Large-scale overexpression	12
3.1.6. FPLC purification by affinity chromatography.....	13
3.1.7. FPLC purification by size-exclusion chromatography.....	13
3.2. PROTEIN PHOSPHATASE 1 ALPHA (PP1 α)	14
3.2.1. PP1 constructs.....	14
3.2.2. Overexpression.....	15
3.2.3. Low-scale purification	16
3.2.4. FPLC purification by affinity chromatography.....	16
3.2.5. FLPC purification by size-exclusion chromatography.....	17
3.3. CHARACTERIZATION OF THE INTERACTION PP1 α - CASPASE 9.....	17
3.3.1. Pull-down assay.....	17
3.3.2. Western blot analysis	18
3.3.3. Biolayer Interferometry (BLI)	18

3.3.4.	Isothermal Titration Calorimetry (ITC)	20
4.	RESULTS AND DISCUSSION	20
4.1.	LOW-SCALE PURIFICATION	20
4.1.1.	Caspase 9	20
4.1.2.	PP1 α	22
4.2.	CASPASE 9 FPLC PURIFICATION	22
4.2.1.	Affinity chromatography	22
4.2.2.	Size-exclusion chromatography	24
4.3.	PP1 α FPLC PURIFICATION	27
4.3.1.	Affinity chromatography	27
4.3.2.	Size-exclusion chromatography	28
4.4.	INTERACTION STUDIES BETWEEN CASPASE 9 AND PP1 α	29
4.4.1.	Pull-down assay between caspase 9 and PP1	29
4.4.2.	Biolayer Interferometry (BLI)	31
4.4.3.	Isothermal Titration Calorimetry (ITC)	33
5.	CONCLUSIONS	36
6.	BIBLIOGRAPHY	37

INDEX OF FIGURES

Figure 1. Caspase family members..	2
Figure 2. Caspase-dependent apoptosis pathway	3
Figure 3. Schematic 3-dimensional representation of Δ CARD caspase 9..	4
Figure 4. Ligation independent cloning (LIC) method	7
Figure 5. Squematic representation of the pET23b(A) and pETGKI vectors	9
Figure 6. Squematic representation of site-directed mutagenesis technique.	10
Figure 7. The technique is based on the affinity of the ligand for the matrix..	11
Figure 8. A)RP1B-PP1alpha vector. B) pGro7 vector encoding GroEL/ES chaperone	15
Figure 9. Pull-down assay technique.....	17
Figure 10. Experimental steps in a Biolayer Interferometry (BLI) sensogram	19
Figure 11. 10% polyacrylamide gel of the expression of CARD(A) and caspase 9 constructs Δ CARD4QC, Δ CARDC287A, FLC287A	21
Figure 12. 10% polyacrylamide gel of the low-scale purification of T125D (lane 1 and 2) T125E (lane 3 and 4), S196D (lane 5 and 6), and C9WTFL(last lane)	21
Figure 13. A).10% polyacrylamide gel of the expression of PP1 α 7-330. B) 10% polyacrylamide gel of the expression of PP1 α 7-300.	22
Figure 14. (A) 10% polyacrylamide gel of the affinity purification of CARD and Δ CARDC287A (B) Concentrated fraction of the FLC287A pure protein.	23
Figure 15. 10% polyacrylamide gel of the affinity purification caspase 9 mutants. From left to right T12D, T125E and S196D pure protein, respectively.....	23
Figure 16. C9WTFL Chromatogram of size-exclusion chromatography.....	24
Figure 17. 10% polyacrylamide gel of the affinity purification of his-tagged caspase 9 (C9WTFL) ..	24
Figure 18. Chromatogram of size-exclusion chromatography of PP1+CARD.....	25
Figure 19. 10% polyacrylamide gel of the size-exclusion chromatography of CARD.....	25
Figure 20. 10% polyacrylamide gel of the SEC of Δ CARDC287A and PP1	26
Figure 21. Chromatogram of size-exclusion chromatography of C9WTFL.....	26
Figure 22. 10% polyacrylamide gel of the size-exclusion chromatography of C9WTFL.....	26
Figure 23. Chromatogram of size-exclusion chromatography of PP1.....	27
Figure 24. FLPC chromatogram of PP1 α 7-330 using a 5 mL His-Trap column	27
Figure 25. 10% polyacrylamide gel of the fractions of the chromatogram shown in Fig.12	28
Figure 26. Chromatogram of the size-exclusion chromatography of PP1 α 7-330.....	28

Figure 27. 10% polyacrylamide gel of the fractions of the size-exclusion chromatography	29
Figure 28. A) Western blot revealed with Anti-GST antibody. B) Western blot revealed with Anti-His antibody	29
Figure 29. 10% polyacrylamide gel of the pulldown assay using GST beads , pure PP1 as prey and pure C9C287AFL as bait.....	30
Figure 30. Kinetic assay using Ni-NTA sensors	31
Figure 31. Kinetic assay using Ni-NTA sensors	32
Figure 32. Combinatorial-control model of the catalytic subunit of protein phosphatase 1 (PP1c) proposed by Bollen (2001)	33
Figure 33. ITC for PP1 and C9WTFL.	34
Figure 34. Schematic representation of the interplay between the kinase AKT, phosphatases PP1 and PP2A and caspase 9 , the last initiator caspase in the apoptotic pathway.	35
Figure 35. Caspase 9 sequence fragment	36

ABRREVIATIONS

μl: microliter

Apaf-1: apoptosis protease-activating factor-1

ATP: adenosin triphosphate

Bad: Bcl-2-associated death promoter

Bcl-2: protein derived from B-cell lymphoma

BLI: Biolayer interferometry

BLITz: bliolayer interferometry technology (device)

C9: caspase 9

CARD: caspase activation recruitment domain

CCD: charged couple device

CDK1: Cyclin-dependent kinase 1

dATP: deoxyadenosine triphosphate

DED: death effector domain

DNA: deoxyribonucleic acid

dNTP: deoxynucleotide triphosphate

dTTP: deoxythymine triphosphate

EDTA: Ethylenediaminetetraacetic acid

ERK: extracellular-signal-regulated kinase

FL: full length

FPLC: fast protein liquid chromatography

GST: glutathione S-transferase

HRP: horseradish peroxidase

IAP: inhibitors of apoptosis

IPTG: isopropil - β - D - tiogalactopiranósido

ITC: isothermal titration calorimetry

K_D: dissociation constant

LB: Luria Broth (medium)

LIC: Ligation independent cloning

Ni-NTA: níquel nitroacetic acid

OD: optical density

PAGE: polyacrylamide gel electrophoresis

PBS: Phosphate buffered saline

PCR: Polimerase chain reaction

PIP: PP1-interacting protein

PMSF: phenylmethylsulfonyl fluoride

PP1: protein phosphatase-1

PP2A: protein phosphatase 2 A

PRK: protein c-related kinase

SDS: sodium dodecyl-sulfate

SEC: Size-exclusion chromatography

TBST: Tris-Buffered Saline and Tween 20

TEV: tobacco etch virus

T_m: MENTING TEMPERATURE

WT: wild type

1. INTRODUCTION

1.1. APOPTOSIS

Apoptosis is a highly regulated form of programmed cell death that eliminates individual cells in a controlled way, playing a key role in the maintenance of tissue homeostasis. As a natural process involved in normal development, it controls cell number and proliferation. During morphogenesis, this process eliminates unneeded cells to form functional tissues and organs. Apoptosis is also important in normal tissue physiology, for example, as part of the regular renewal of cells in the intestine or bone marrow.

Stress and DNA damage usually trigger apoptosis. However, apoptotic cell death is deregulated in some conditions, having devastating effects in the organism. Insufficient or untimely cell death can result in cancer or autoimmune disorders, while accelerated cell death is evident in acute and chronic degenerative diseases, immunodeficiency and infertility (reviewed by Hassan *et al*, 2014). In fact, one of the hallmarks of cancer cells is resistance to apoptosis, which is acquired through different mutations that alter different control points in the apoptotic pathway. For this reason, it is crucial to understand the molecular events that lead to the dysregulation of apoptosis in cancer and some other pathologies.

Apoptosis is different from other cell death processes because it is designed to ensure a safe and controlled dismantling of the cell, thus minimizing collateral damage within the tissue. The cellular changes that constitute the apoptotic program proceed according to a precisely coordinated schedule. From an outside view, patches of the plasma membrane herniate to form structures known as blebs. The nucleus collapses into a dense structure and the chromosomal DNA is cleaved into small fragments. Finally, usually within an hour, the apoptotic cell breaks up into small fragments sometimes called apoptotic bodies, which are rapidly ingested by phagocytosis. (Weinberg *et al.*, 2007)

Inside the cell, lots of cellular events take place. At the level of proteome, hundreds of proteins undergo restricted proteolysis during apoptosis. It has been shown that members of a family of proteases with specific cellular target called caspases are responsible of this to a great extent (Taylor *et al.* 2008). There are two studied apoptosis pathways: intrinsic and extrinsic pathways that eventually converge in the apoptotic caspase dependent pathway.

1.2. CASPASES

1.2.1. Caspases and its role in apoptosis

Caspases are a family of cysteine aspartatyl-specific proteases which play a key role in apoptotic cell death. They induce controlled cell death by cleaving target cellular proteins in specific aspartic residues.

Caspases are necessary for apoptosis and inflammatory response (Denault and Salvesen, 2001). There are 14 different types of caspases in mammals but only 11 of them are present in humans. They are produced in the cell as inactive zymogens (Figure 1).

The zymogens consist of an N-terminal prodomain and a catalytic domain (30kDa) with a large subunit (20kDa) and a small subunit (10kDa). All solved crystallographic structures show the same basic folding.

The catalytic domains of the different caspases are well conserved among caspases. The catalytic site, also highly conserved among this family of proteases, comprises two residues His²³⁷/Cys²⁸⁵ that are part of the large subunit. However, the responsible for the substrate specificity of caspases is the variation in the amino acid sequence of the small subunit.

The amino-terminal region of caspases contains two other domains: caspase activation and recruitment domain (CARD) and death effector domain (DED) whose function is related with caspase regulation, detailed later in this section.

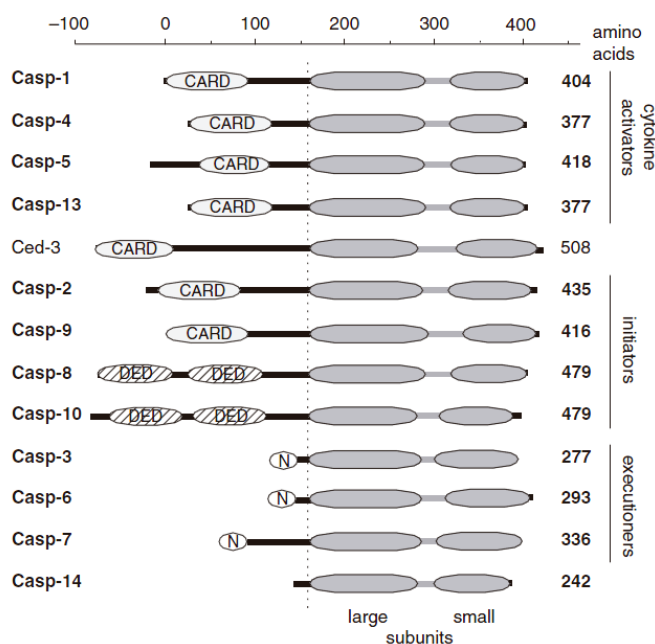


Figure 1. Caspase family members. Schematic representation of human caspases along with Ced-3 from *C. elegans*. The three groups (i.e., cytokine activators, initiators, and executioners) are based on demonstrated or presumed physiological functions. CARD domain (light gray), DED domain (hatched), and the small N-peptide of executioner caspases are also depicted in the diagram. The scale is set in accordance to caspase-1 numbering and the dotted line indicates the starting point of the large subunit (dark gray; amino acid 161 in caspase-1). Domains were delineated using the conserved domain database (CDD) and the Pfam algorithm. (Denault and Salvesen, 2001).

The activation process is initiated by extracellular or intracellular cell death signals. They provoke the aggregation of intracellular adaptor molecules that can activate procaspases. The activation of caspases is regulated by members of the Bcl-2 and IAP (inhibitor of apoptosis) protein families. (Figure 2)

Caspases are classified in two main groups according to its role: initiators and executors. The initiator caspases are the first signal transducers and they are activated by autoproteolysis under certain stimuli. Once initiator caspases are activated, they amplify the signal by cleaving executor caspases, thus activating them. The effector caspases can act over a large range of cellular targets. From this point on, the amplification of the signal is exponential and death execution is irreversible (Qin *et al.*, 1999).

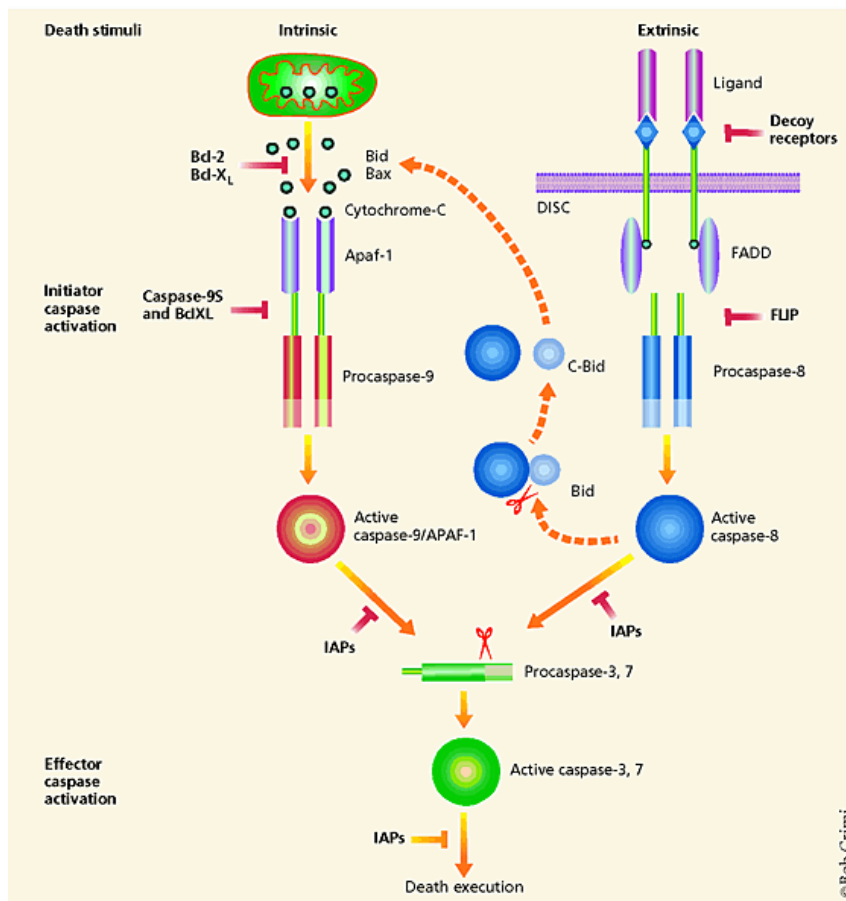


Figure 2. Caspase-dependent apoptosis pathway (Zeng and Flavell, 2010).

1.2.2. Caspase 9

Caspase 9 is the last initiator caspase in the caspase-dependent apoptotic pathway. Its activation by dimerization requires loop rearrangement for the correct orientation of the catalytic machinery and the substrate binding sites (Denault and Salvesen, 2001).

The activation of procaspases usually requires cleavage through specific aspartyl residues that are present in two sites: the linker between the prodomain and the catalytic region and the one between the large and the small subunit. The scission releases the prodomain and generates both large and small subunits. Caspase 9 has two potential sites for processing, aspartic residues 315 and 330 and the active site, the 287 cysteine residue. The mutation of the active site impedes autoprocessing and the generation of the two subunits (Srinivasula *et al.*, 1998).

Δ CARD caspase 9 structure shows a heterotetramer that consists of two antiparallel heterodimers, each of them composed by a p35 subunit (35 KDa) and a p10 subunit (10 KDa).

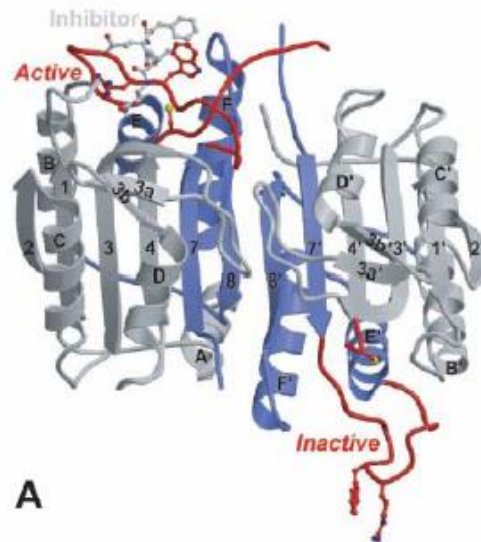


Figure 3. Schematic 3-dimensional representation of Δ CARD caspase 9. The structure of caspase 9 without CARD domain consists of two domains. The large subunit is represented in grey and the small in blue. The inhibitor molecule, the lateral chains of Cys 285 catalytic residue and the residues that determine the specificity /Arg 341 and Trp 340 are represented as spheres and sticks. In red, big deviations between catalytic residues and determinant of the domain specific are observed. (Renatus *et al.*, 2001).

Caspase 9 is not activated by proteolysis as other caspases. It is activated by homophilic interactions between the CARD domain of caspase 9 and Apaf-1 cofactor in the presence of cytochrome c and ATP, generating a completely functional apoptosome. The apoptosome controls apoptotic response to lethal agents for cell, such as ionizing radiation or chemotherapeutic drugs.

Apoptosome oligomerization results in dimerization of caspase 9, increasing local concentration above the K_D (dissociation constant). Alternatively, Apaf-1 in the active conformation generates Caspase 9 monomer, providing a complementary surface that simulates the dimerization interface. Somehow, caspase 9 activation resembles members of the trypsin family of serine proteases.

Active caspase 9 is able to process and activate caspases 3, 6 and 7, thereby transmitting apoptosis signal to the execution phase (Renatus *et al.*, 2001). Due to its function, caspase 9 represents a molecular target in cancer therapy strategies and it has been extensively studied.

1.2.3. Regulation of caspases

Given the function of caspases, they appear as a potential threat to every cell and a failure in modulating caspase activity results in aberrant or untimely apoptotic cell death, potentially leading to carcinogenesis, autoimmunity, neurodegeneration and immunodeficiency (reviewed in Parrish *et al.* 2013). Therefore, their activation needs to be tightly and efficiently regulated. Although the

complicated regulatory mechanism has not been totally elucidated, there are some well-described control points.

As mentioned above, they are synthesized as zymogens, which mean that they are initially produced in an inactive form, lacking protease activity. The final goal of this “biological restriction” is that they will only be activated under certain stimuli at a particular time and space.

Another form of regulation is proteolysis, in which the N-terminal prodomain has an important role. This region contains well-conserved domains: CARD for caspases 1,2,4,5,9,11 and 12, and DED found in caspase 8 and 10 (Figure 1). Both domains are distantly related and are implicated in homophilic interactions with other proteins, allowing caspase zymogens to be recruited to protein complexes to promote their activation. Caspases containing CARD or DED domains are usually activated by proteolytic cleavage with the exception of caspase 9, as described before (Denault and Salvesen, 2001).

Apoptosis is also regulated by reversible protein phosphorylation that acts as a molecular switch and represents a last control point in caspase 9 regulation. This posttranslational modification consists in the addition or removal of a phosphate group (negatively charged) in a protein residue. This mechanism is controlled by two big families of proteins: protein kinases and protein phosphatases. Phosphorylation/dephosphorylation events affect the conformation of the target protein and/or its interaction with other proteins, as well as its activity, function, half-life, stability, substrate affinity or subcellular localization (Figureido *et al*, 2014).

In eukaryotes, the most commonly modified residues are serine and threonine. In fact, 98% of dephosphorylation occurs at these two amino acids and there are two major proteins of the family of Phosphoprotein Phosphatases (PPP), named Protein Phosphatase 1 (PP1) and Protein Phosphatase 2A (PP2A), that account for 90% of serine/threonine dephosphorylation (reviewed by Xiao *et al*, 2010). PP1 and PP2A are in fact important regulators at several levels of the apoptotic pathway and they are two of the most abundant enzymes in many cell types. They are part of a complicated interplay between kinases and phosphatases in the execution of apoptosis, in which caspases are the major drivers.

1.3. PROTEIN PHOSPHATASE 1

Protein phosphatase 1 (PP1) is an ubiquitous serine/threonine phosphatase that regulates different important cellular processes such as cell progression, cytokinesis, transcription, protein synthesis, carbohydrate metabolism, muscle contraction and neuronal signaling.

PP1 is a highly conserved 38 kDa protease that dephosphorylates hundreds of crucial biological targets, and its apoenzyme associates with more than 200 regulatory proteins to form specific holoenzymes (Bollen *et al* 2010). In fact, the specificity of the catalytic domain for certain residues near the target phosphorylation site appears to be limited. For this reason, the action of PP1 is directed in time and space by these regulatory proteins. However, PP1 has shown to possess interaction domains which are conserved among its interacting partners. The most common one is the RVxF motif which is present in most PP1-interacting proteins (PIPs). The consensus sequence

described by Bollen (2001) is K/R/H/N/S-V/I/L-x-F/W/Y, being x any residue except Phe,Ile,Met,Tyr,Asp or Pro. Although it brings about little conformational changes on the catalytic subunit of PP1, the binding to this motif is crucial for the partner proteins to become anchored to PP1. This docking site helps to bring closer interacting proteins, thereby making additional interactions possible, thus determining the activity and substrate specificity of the holoenzyme. The disruption of only a single motif can be enough to weaken or even break the interaction. Other common PIPs interaction motifs are SILK and MyPhoNe, both usually N-terminal to the RVxF motif.

Serine/Threonine protein phosphatases PP1 and PP2A participate in a complicated regulatory crosstalk between kinases, phosphatases and their targets at several points of the apoptotic signaling pathway. PP1 and PP2A can present both an anti-apoptotic and apoptotic function (Li *et al.*, 2006 and Dohoney *et al.*, 2004). Also, the inhibition of PP1 α or PP2A can trigger apoptosis which suggests their role as anti-apoptotic proteins under certain conditions (Singh *et al.*, 2000 and Kang *et al.*, 2001). In contrast, PP1 and PP2A have also been described as apoptosis enhancers through several actions. Both proteins stimulate mitochondrial release of cytochrome C, which is a primary event in apoptosis intrinsic pathway. Furthermore, these two proteins induce apoptosis by dephosphorylating Bad, a pro-apoptotic Bcl-2 family member (Van Hoof *et al.*, 2003 and Ayllon *et al.*, 2000).

PP1 and PP2A can also control apoptosis through negative regulation of anti-apoptotic partners, modulating Akt function as regulator of cell survival, differentiation and gene expression by directly dephosphorylating Thr 308 and Thr 450 and Ser 473, respectively (Figure 2) (Kuo *et al.*, 2008 and Xiao *et al.*, 2010). These two phosphatases play an important role in the regulation of caspase 9 phosphorylation state, thus controlling its activation under certain stimuli.

1.4. PP1 - CASPASE 9 INTERACTION IN CASPASE-DEPENDENT APOPTOTIC PATHWAY

Dessauge *et al.* (2006) have demonstrated that PP1 α directly dephosphorylates caspase 9, activating it, what promotes its protease activity and the irreversible cell entry in apoptosis.

The interaction was first determined by immunoprecipitation of cell extracts and pull-down assays. Overlapping peptides covering the sequence of Caspase 9 were synthesized in a nitrocellulose membrane, hybridized with PP1 and revealed with Anti-PP1 in a Far Western Blot assay, showing two binding sites. The first site corresponded to the first CARD domain (1-92) residues and the second site was identified in the catalytic subunit of Δ CARD domain (140-416). Both sites are exposed in the three-dimensional structure being accessible for the interaction with PP1. The same experiment was performed synthesizing PP1 overlapping peptides hybridized with caspase 9 and revealed with Anti-caspase9, showing three binding sites to Caspase9.

In the present work, we have studied the *in vitro* interaction between caspase 9 and PP1 fusion proteins using biophysical techniques. The aim is to understand the role of this interaction in the regulation of the apoptotic pathway. After the phosphorylation sites described in the literature phosphorylated by known kinases such as Erk, CDK1, and Akt, we designed three phosphomimicking mutants to elucidate the caspase 9 dephosphorylation site mediated by PP1.

2. OBJECTIVES

- Cloning of several constructs of caspase 9 in pETGKI vector.
- Overexpression in *E. coli* and purification of several human caspase 9 and human PP1 constructs as stable fusion proteins.
- Study of the interaction between caspase 9 and PP1 *in vitro* using biophysical techniques.
- Design of caspase 9 phosphomimetic mutants and evaluation for the interaction with PP1.

3. MATERIALS AND METHODS

3.1. CASPASE 9

3.1.1. Cloning

The final goal is to overexpress the protein in a sufficient amount for further purification steps and interaction studies with PP1.

The insert of caspase 9 wild type full-length (C9WTFL) cloned in the pET23b vector was gently handed over by Enrique Pérez-Payá laboratory, CIPF. Several constructs of caspase 9 were cloned to overexpress different domains of the protein (see Table 1 in Appendix). Caspase 9 constructs were cloned in pETGKI vector, an in-house modified version of the pET28-NKI/LIC 6His/3C vector (originally obtained from Dr A. Perrakis group, NKI, Amsterdam) in which the His tag was substituted by a GST tag.

The cloning method used was Ligation Independent Cloning (LIC), detailed in **¡Error! No se encuentra el origen de la referencia..** LIC is a cloning system that uses the 3'→5'-activity of T4 DNA polymerase to create 10-15 base single complementary overhangs in both vector and insert. Vectors are linearized by PCR or restriction enzyme digestion and inserts are amplified by PCR.

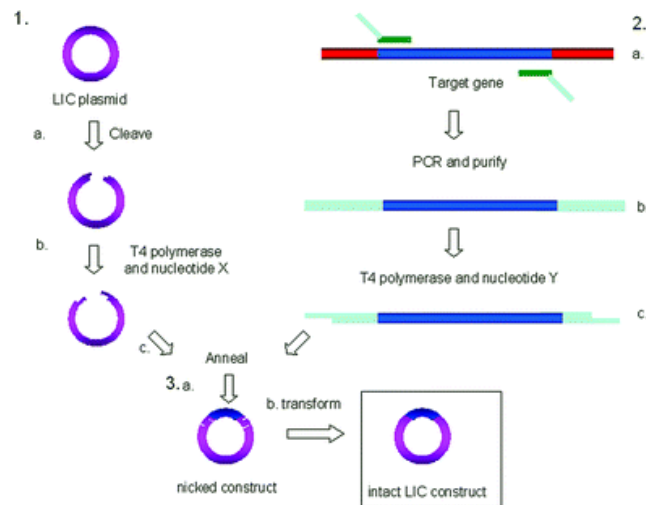


Figure 4. Ligation independent cloning (LIC) method. First step is the digestion of the recombinant vector with a restriction enzyme (1a) and subsequent treatment with T4 polymerase, adding the nucleotide dTTP (1b) for generating cohesive ends

compatible with the insert. In parallel, the insert is amplified with primers designed to perform the LIC strategy (2a) and then it is purified (2b) and treated with T4 polymerase and nucleotide dATP (2c). Ligation (3a) is produced simply by mixing insert and vector. The resulting recombinant vector is transformed into the appropriate system (3b) (Bonsor et al, 2006)

First, the vector was linearized using the pETGKI KpnI restriction site (Figure 5B). It was digested for 6 h at 37°C by mixing 30 µl of the purified plasmid (Miniprep) with 2 µl of KpnI enzyme (New England Biolabs®), 4 µl of buffer 1 (New England Biolabs®), 0.4 µl of Bovine Serum Albumin (New England Biolabs®), and 3.6 µl of milliQ water.

The different inserts were amplified using polymerase chain reaction (PCR). The PCR conditions used for all the constructs are described in Table 2 (Appendix). The primers used for each construct are described in Table 1 (Appendix) and their sequences are detailed in Table 3 (Appendix).

In order to confirm that the amplification was successful and the inserts had the proper size, a 1% agarose (Pronadisa®) gel was prepared using TAE 1X buffer (40mM Tris, 20mM acetic acid, and 1mM EDTA) and 2,5 µl of GelRed (Biotium®). 3 µl of each sample and 2 µl of Blue 6X Loading Dye were loaded. The molecular marker used was DNA Ladder 1 kb (Nippon®). The electrophoresis was performed at 100V in a Biostep® cuvette for 40 minutes. The presence of the inserts was confirmed under UV light. Then, inserts were purified using NucleoSpin® Gel and PCR Clean-up (Macherey-Nagel).

Then, vectors and inserts were treated separately with T4 DNA polymerase prior to the ligation reaction. 15.3 µl of vector/insert were mixed with 4 µl of T4 DNA polymerase buffer, 0.2 µl of T4 DNA polymerase and 0.5 µl of dATP (insert) or dTTP (vector). Reactions were incubated for 10 minutes at room temperature and 10 minutes at 70°C in a thermoblock (Eppendorf®). During this step reaction, the incorporation of a dNTP limits the exonuclease processing and creates a balance between exonuclease and polymerase activities of T4 DNA polymerase. In each reaction a complementary dNTP is added as indicated above. The final goal is to obtain complementary overhangs of the same nucleotide type, adenine for inserts and thymine for vectors.

Finally, pETGKI vector and the appropriate insert in a 1:1 proportion were incubated for 5 minutes at room temperature. Thus, the complementary overhangs created by T4 polymerase were annealed simply by mixing insert and vector. To stop the reaction, 2 µl of EDTA 50mM were added and incubated for 10 minutes at room temperature.

This ligation method presented several advantages, as restriction enzymes or ligase are not needed, unlike traditional systems. Although joined fragments usually have nicks, they are repaired by *E.coli* during transformation. This process is very efficient and creates scarless recombinant plasmids.

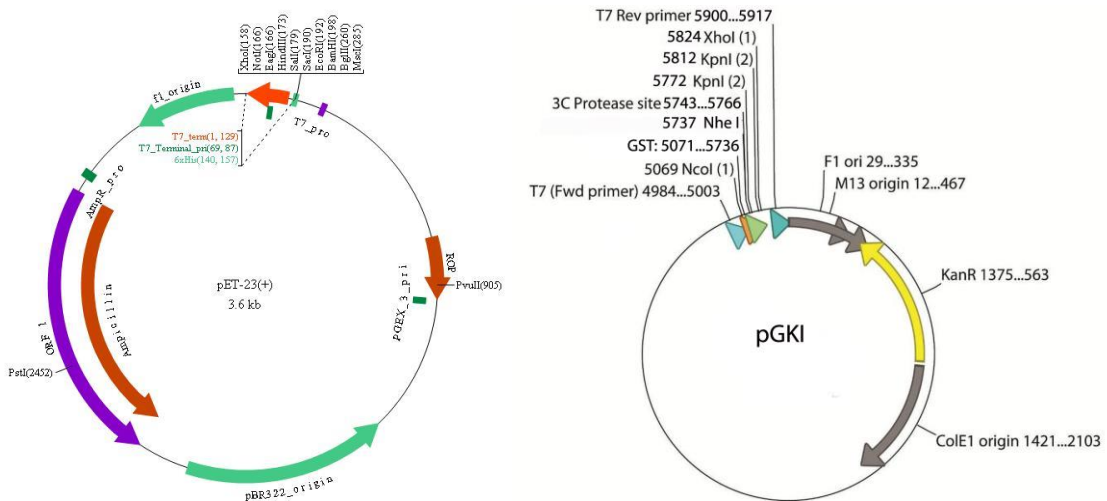


Figure 5. Schematic representation of the pET23b(A) and pETGKI vectors. Binding sites of the primers are shown as well as the 3C protease and XhoI, KpnI and NcoI restriction enzymes cleavage sites.

Next step was heat shock transformation in DH5 α *E. coli* (Stratagene[®]), a strain specifically used for cloning. DH5 α strain increments insert stability and improve the extracted DNA plasmid. For this purpose, chemically competent cells were thawed on ice for 5 minutes. Then, the ligation reaction was added to the cells and incubated on ice for more than 10 minutes. For the heat shock, cells were incubated at 42^oC during 1 minute and 30 seconds and tubes were placed on ice to reduce cell damage. Then, cells were incubated with 200 μ l of LB medium without antibiotics at 37^oC. This step is crucial for the cells to recover and express antibiotic resistance. After 1 hour of incubation, cells were plated in a Petri dish containing LB agar supplemented with 33 μ g/mL kanamycin and were incubated overnight at 37^oC.

After this procedure, a colony PCR (Table 4 in Appendix) was performed in order to check whether the colonies had the vector and the insert was successfully incorporated. Positive colonies were cultured in 5 ml of LB medium supplemented with 33 μ g/mL kanamycin overnight at 37 ^oC and the plasmid was extracted with QuickGene Plamid Kit S II (Fujifilm) for sequencing analysis (Biomedicine Institute of Valencia sequencing service).

3.1.2. Site-directed mutagenesis

Recombinant protein overexpression in prokaryotes usually involves lack of most post-translational modifications. Facing the possibility that this could have a negative impact in the caspase 9- PP1 interaction, a phosphomimetics approach was design. Phosphomimetics consists of amino acid substitutions that in most cases mimic a phosphorylated protein.

This modification was carried out by *in vitro* site-directed mutagenesis (Figure 6). This technique was used to change a single amino acid in the sequence of C9WTFLL construct. Based on literature, three residues were chosen as candidates for the phosphorylation: threonine 125 was changed for a glutamic acid (T125E) and serine 196 was changed for an aspartic acid (S196D).

The procedure was performed by Polymerase Chain Reaction (PCR conditions in Table 5, Appendix) in a thermocycler (Eppendorf Mastercycler EPGradient) using KAPA HiFi DNA Polymerase

(Kapa Biosystems®), the supercoiled double-stranded DNA (C9WTFL) and two synthetic oligonucleotides (primer sequence detailed in Table 3, Appendix) containing the desired mutation. The KAPA HiFi DNA Polymerase extends the oligonucleotide primers during the reaction, replicating the plasmid strands with high fidelity. The result is a pool of mutated plasmids containing staggered nicks and the used template plasmid.

Next step is to digest this parental DNA to have only the mutated plasmid. For this purpose, the product is treated with DpnI, a specific endonuclease (target sequence: 5'-Gm6ATC-3') for methylated and hemimethylated DNA. The dam methylation is a characteristic of almost all *E. coli* strain DNA but not of the newly synthesized one. After 1 h of digestion reaction at 37 °C, each mutated caspase 9 vector was transformed in DH5α cells as described previously. The plasmids containing the desired mutation were extracted by miniprep and sequenced as described before.

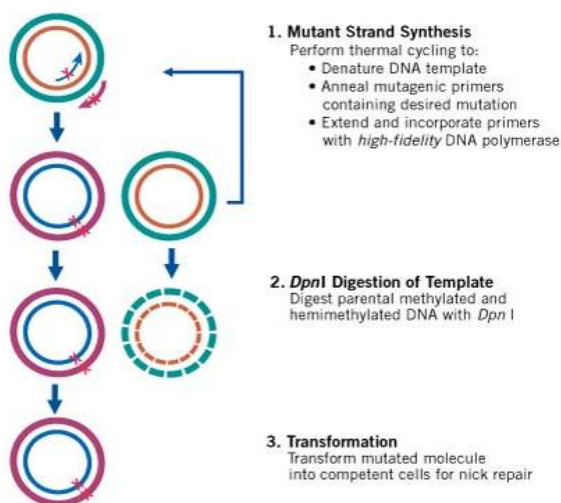


Figure 6. Schematic representation of site-directed mutagenesis technique. Agilent Technologies®, 2015

3.1.3. Low-scale overexpression

The purified plasmid was transformed in BL21 codon plus RIPL chemically competent *E. coli* (Stratagen®) cells as previously described for DH5α cells with the exception of 45 seconds of heat shock incubation. Finally, 150 μL of this cell culture were seeded in a culture plate containing 33.3 μg/ml kanamycin and chloramphenicol (Sigma- Aldrich®) and incubated overnight at 37 °C.

The expression protocol was optimized from Current Protocols in Protein Science, Unit 21.13 (Denault and Salvesen, 2002) including some modifications. An isolated colony of the previously described plate was inoculated in 5 mL of 2xTY medium (16 g tryptone (Pronadisa), 10 g yeast extract (Pronadisa), 5 g NaCl (Panreac) and 1 L distilled water) supplemented with 33.3 μg/mL of kanamycin and chloramphenicol. The cells were cultured overnight at 37 °C in continuous shaking (180 rpm).

Then, the preculture was inoculated in 20 mL of 2xTY medium, supplemented with 33.3 μg/mL kanamycin and chloramphenicol for constructs in pETGKI vector and 100 μg/mL ampicillin and 33.3 μg/mL chloramphenicol for constructs in pET23b vector, and was incubated at 37 °C until the OD₆₀₀

was 0.6. This cellular density corresponds to exponential growth of *E.coli* cells and it is established as the best moment to induce protein overexpression. The absorbance was measured with a cellular densitometer Ultrospec 10 (Amersham Biosciences®). To induce Caspase-9 overexpression, the culture was inoculated with 0.4 mM IPTG (isopropil - β - D - tiogalactopiranoside) (CalBiochem®) and incubated for 4 hours at 30 °C. Finally, cultures were centrifuged (Sorvall ST16R, rotor 75003629) at 4°C and 4000 rpm for 30 minutes. Supernatants were discarded and cells were resuspended in 1 mL PBS (80 mM Na₂HPO₄·7H₂O (Sigma - Aldrich®), 20 mM NaH₂PO₄·H₂O (AppliChem®), 100 mM NaCl (Panreac®), pH 7,4) for each tube. Finally, cells were harvested again by centrifugation at 4°C and 4000 rpm for 20 minutes.

3.1.4. Low-scale purification

Glutathione sepharose beads assays allow the purification of soluble GST-tagged fusion proteins. They consist on a 4% agarose matrix covered by covalently attached glutathione ligand groups. The separation principle is based on affinity chromatography, which depends upon the reversible absorption of biomolecules through biospecific interactions on the ligand (Figure 7). Similarly, Ni-NTA agarose beads assays allow the purification of soluble His-tagged fusion proteins. They consist on a 4% agarose matrix covered by immobilized nickel ions.

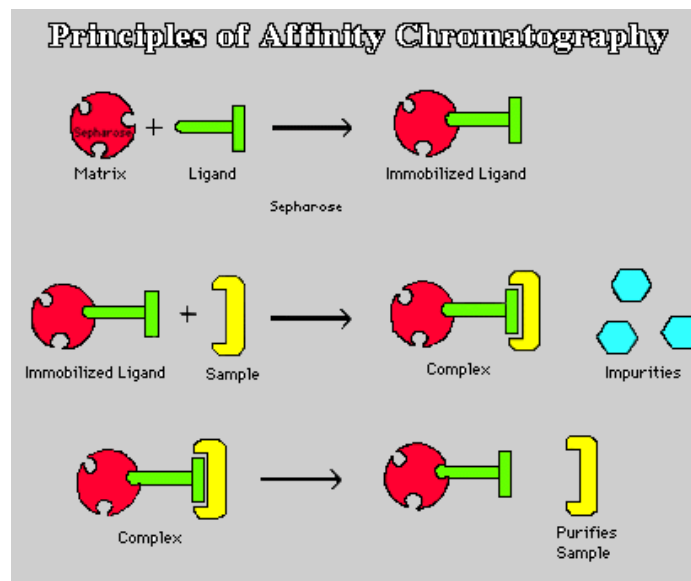


Figure 7. The technique is based on the affinity of the ligand for the matrix. The protein containing a tag is bound by affinity to the covalently attached groups of the resin. Then impurities and proteins unspecifically attached are removed by washing. Finally, the protein is eluted by applying a buffer containing molecules that compete with the sample for the resin (Glutathione or nickel ions) and can be recovered pure.

After caspase 9 overexpression protocol, cells were lysed with 300 μ l of lysis buffer (100 mM Tris pH 8, 200 mM NaCl, 5% glycerol, 0.5% Triton x100 and 1mM PMSF) and the mixture was sonicated using Standard B01010005 (Diagenode®) bioruptor for 30 minutes at 4°C (at 30 seconds intervals). Then, the samples were centrifuged at 4°C at maximum speed during 30 minutes and the supernatant (containing soluble proteins) was kept on ice. Meanwhile, glutathione sepharose 4B

beads (GE Healthcare™) for GST-tagged caspase 9 constructs or Ni-NTA beads (ABT beads) for His-tagged constructs were prepared for the assay.

There are three main steps for affinity chromatography purification. First step is the equilibration of the stationary phase with the appropriate conditions. 80µl of beads in each tube were centrifuged at 6000g for 2 minutes with Sorvall Legend micro 21R (Thermo Scientific®), to remove preservative solution (20% ethanol). Beads were washed and equilibrated with 1 mL milliQ water twice and then, with the same volume of binding buffer (100mM Tris pH 8, 200 mM NaCl, 5% glycerol) two more times. The second step is sample binding and wash. The aim is to attach the target molecules to the resin and wash out the unbound material that will be collected in the flow-through. After centrifugation for 5 minutes at 5000 g, the pellet was resuspended in 300µl milliQ water and incubated at 90°C in Thermomixer comfort (Eppendorf®) for using later as a control. The supernatant was incubated with the beads for 30 minutes in agitation at 4°C. Then, the mixture was centrifuged for 5 min at 4000 g to remove all the unbound proteins by pipetting the supernatant (flow-through control). At this point, beads are loaded with the desired fusion protein. Then, beads were washed with 1 mL binding buffer twice. Last step was elution, in which biomolecules are released from the biospecific ligand into 100 µl elution buffer (Ni-NTA:100mM Tris pH 8, 200 mM NaCl, 5% glycerol, 200mM imidazole; Glutathione sepharose 4B: 100mM Tris pH 8, 200 mM NaCl, 5% glycerol, 20mM reduced glutathione).

After elution, samples were prepared for SDS-PAGE electrophoresis. For this, 40µl of pellet, supernatant, flowthrough and wash (as controls) and 40µl of elution were mixed with 15µl SDS-PAGE loading buffer 6X. Samples were incubated at 95°C in Thermomixer comfort (Eppendorf®) for 10 minutes to denature the protein. Then, 10µl of each sample and 2µl of molecular weight Blue Star Prestained Protein Marker (Nippon®) were loaded into a 10% polyacrylamide gel. The gel was run for 40 minutes at 200 V in a Mini-Protean tetra cell electrophoresis (Biorad®) tray. The electrophoresis buffer used was NuPAGE® MES 1X (Invitrogen®). Then, the gel was dyed with a Coomassie Blue solution (1g Coomassie Blue, 40% methanol, 10 % glacial acetic acid and 50% distilled water). After 5 minutes dyeing, the gel was destained with Coomassie blue destaining solution (10% methanol, 10% glacial acetic acid, 80% of H₂O) until the protein band was visible. The presence of the purified protein allowed us to continue with the large scale purification experiments.

3.1.5. Large-scale overexpression

The protocol was essentially following the low-scale overexpression protocol but scaling volumes. The transformed cells were inoculated in 50 mL 2xTY culture medium supplemented with 33 µg/mL kanamycin and chloramphenicol and after the incubation time, this preculture was inoculated in 1 L 2xTY medium, supplemented with the same antibiotics. Also, cultures were centrifuged in a Beckman coulter J6, rotor JS-4.2A centrifuge at 4°C and 3600 rpm during 1 hour. Cells were resuspended in 40 mL PBS (80 mM Na₂HPO₄·7H₂O, 20 mM NaH₂PO₄·H₂O, 100 mM NaCl, pH 7.4) for each liter of culture and transferred to a 50 mL tube. Finally, cells were harvested by centrifugation for 20 minutes at 4000 rpm (Sorvall ST16R, rotor 75003629) and kept at -20 °C for further purification steps.

3.1.6. FPLC purification by affinity chromatography

The purification was performed using the cell pellet obtained after the overexpression of each caspase 9 construct, kept at -20 °C. The pellet was thawed on ice and resuspended in 50 mL of lysis buffer (100 mM Tris pH 8, 200 mM NaCl, 5% glycerol, 0.5% Triton X-100, half tablet of complete EDTA-free protease inhibitor cocktail (Roche®)). The dissolved pellet was sonicated for 30 minutes (1 second On-1 second OFF), in a Bioblock scientific Vibra Cell 75042 sonicator. The solution was centrifuged at 17000 rpm for 30 minutes at 4°C (Sorvall RC6, SS-34 rotor).

Caspase 9 constructs with GST tag were purified using a GST-Trap™ 5 mL column (ABT Agarose Beads Technologies®) and caspase 9 constructs with a His tag were purified using a Ni-NTA column. Supernatant was filtered through a syringe filter of 0.45µm diameter and passed through the columns using a Gilson Minipuls 3 peristaltic pump. The column was previously equilibrated with two washes, first with 5 column volumes of milliQ water and then with 5 column volumes of buffer A in both cases (100 mM Tris pH 8, 200 mM NaCl, 5% glycerol).

Last step was the elution of the column to obtain the desired protein. For GST-tagged constructs, the column was initially washed with approximately 20 mL of buffer A. Then, the sample was eluted with 12 mL of buffer B (100 mM Tris pH 8, 200 mM NaCl, 5% glycerol, 20mM Glutathion) in three fractions. For His-tagged constructs, the column was washed with 40 mL of buffer B and the protein was eluted with a buffer B(His: Tris 100 mM pH 8, NaCl 200 mM, 5% glycerol, 200 mM Imidazole) gradient using the Äkta purifier (GE Healthcare).

Three samples were used as a control: the discarded pellet obtained after lysate centrifugation (to check if the protein was expressed insoluble), the flow-through of the column (to check that the protein of interest has been retained in the column) and a fraction of the posterior wash. These samples and the elution fractions were prepared and run as described in Material and methods 3.1.4.

According to the electrophoresis results, the fractions containing the desired pure protein were concentrated by centrifugation (Eppendorf Sorvall ST16R) at 4000 rpm and 4°C using a Amicon® Ultracel 30K cutoff concentrator for CARD, ΔCARD and C9C287A constructs and a 3K concentrator for C9WTFL and all the mutant constructs derived from it, until the volume was 1.5 mL.

3.1.7. FPLC purification by size-exclusion chromatography

Size-exclusion chromatography (SEC) is a method in which proteins or other molecules are separated based on their size and molecular weight. This is an additional step to get pure protein, free of any contaminant that may interfere with further interaction studies.

SEC was performed using the Äkta Prime equipment with a Superdex 200 26/60 column (Pharmacia Biotech®). The column was equilibrated with 360 ml of SE buffer (20mM Tris pH 8, 200 mM NaCl, 5% glycerol, 1 mM β-mercaptoethanol) and 2.5 mL of the eluted protein from the affinity chromatography were injected into the system to perform the separation.

The fractions containing a peak in the chromatogram were run in a 10% polyacrylamide gel as described before and the fractions containing the desired protein were concentrated using a new Amicon® Ultracel 30K or 3K concentrator, depending on the construct, until the concentration was enough to perform the interaction assays.

This is the general protocol once the purification of both caspase 9 and PP1 were optimized. At the beginning of the project caspase 9 (CARD and Δ CARD C287A constructs) and PP1 were copurified in size-exclusion chromatography in order to favor the stability of PP1 due to the interaction. The sample containing caspase 9 and PP1 was concentrated to a final volume of 2.5 mL and injected in size exclusion chromatography, using a 200 26/60 column.

As the protein cannot be frozen without losing its stability, this purification protocol was repeated every time an interaction assay was performed.

3.2. PROTEIN PHOSPHATASE 1 ALPHA (PP1 α)

3.2.1. PP1 constructs

The human genome contains three different genes that encode four distinct catalytic subunits of PP1: PP1 α , PP1 β/δ and the splice variants PP1 γ 1 and PP1 γ 2. Two different constructs of PP1 α were used to overexpress it as a fusion protein in *E.coli*.

The PP1 α sequence full length is 990 base pairs, which encodes a 38 kDa protein of 330 amino acids. The first PP1 crystallization studies in 1995 showed that only 7-300 residues were observed in the electron density maps of the solved structure, although PP1 $_{\alpha 1-330}$ was crystallized, showing that N and C terminal of the protein are disordered. Only in the structure of MYPT1:PP1 residues 301-309 have been observed in the solved structure. In this work, we started working with PP1 $_{\alpha 7-330}$ and PP1 $_{\alpha 7-330}$ in parallel but finally we used the PP1 $_{\alpha 7-330}$ construct, as we managed to optimize its purification.

PP1 $_{\alpha 7-330}$ construct

The vector used for the expression of PP1 was RPB1-PP1 α vector (Addgene plasmid #51768), which encodes the PP1 $_{\alpha 7-330}$ sequence in frame with an N-terminal Thio₆-His₆ expression and purification tag (MGSDKIH HHHHH) and a TEV cleavage site (ENLYFQGH) (Peti and Page, 2007). The TEV cleavage site allows the purification tag to be cleaved for further purification steps and structural studies. This vector has also a kanamycin resistance gene. The other vector used for the expression of PP1 was the pGRO7 plasmid (Chaperone Plasmid Set, Cat#3340, Takara) encoding the chaperone GroEL/GroES (Figure 8).

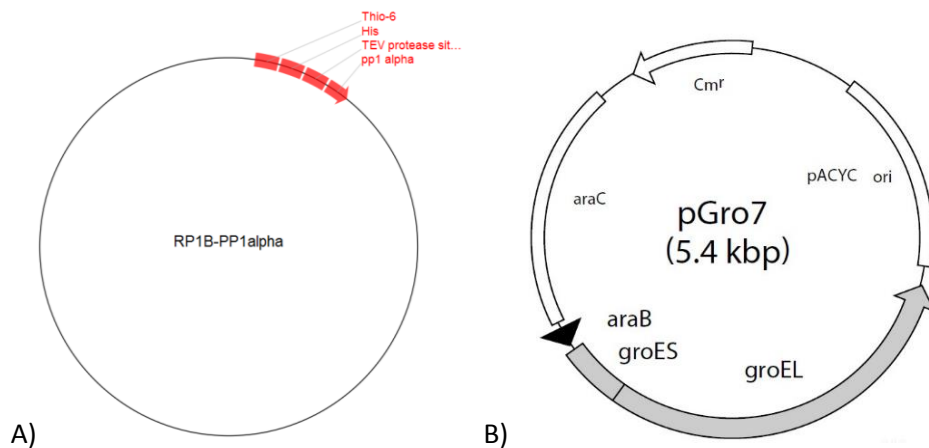


Figure 8. A) RPB1B-PP1alpha vector. B) pGro7 vector encoding GroEL/ES chaperone

These two vectors were cotransformed by heat shock bacterial transformation into chemically competent BL21 *E.coli* cells as described for caspase 9 constructs. The difference is that this time two vectors were co-transformed simultaneously.

PP1_{α7-300} construct

The RPB1-PP1_α vector (Addgene plasmid #51768) was modified in order to encode a shorter version of the construct of PP1_α: PP1_{α7-300}. This modification was carried out by *in vitro* site-directed mutagenesis using the conditions detailed in Table 6 (Appendix). This technique was performed as described for caspase 9 but introducing a stop codon after the 300 residue. The synthetic oligonucleotides used were PP1_{α3-300} FW and PP1_{α3-300} REV (Table 2 in Appendix).

After 1 h of digestion reaction with DpnI enzyme at 37 °C, the modified RPB1-PP1_α vector was cloned in DH5α as described previously. Positive colonies were sequenced to validate the modification (IBV sequencing service). Then, BL21 cells were cotransformed with the modified RPB1-PP1_α plasmid and the pGRO7 plasmid as described before.

3.2.2. Overexpression

PP1 structural studies were difficult to conduct for many years. The bottleneck was always to have an abundant source of PP1, a sufficient amount of the active, pure and homogeneous enzyme for structural studies. So far, natural sources such as rabbit muscle yield the most active enzyme. However, the purification from natural sources has some important limitations. For example, high quantities of animal tissue are required to obtain enough protein, they yield a mixture of isoforms and studies with mutants are not possible. For this reason, the heterologous expression of PP1 in bacterial cells is very useful. Nevertheless, the production of PP1 in *E.coli* has important problems: it is highly insoluble, exhibits phosphotyrosine phosphatase activity and it is insensitive to regulation by several targeting subunits (reviewed by Peti *et al.* 2013)

In order to solve the problem of insolubility, there are two main strategies. The first one is to fuse PP1 with a tag that increases solubility and the second is *in vivo* refolding. Recently, Peti *et al.*

(2013) developed and optimized a novel PP1 expression protocol that achieves a 10-fold increase in PP1 yield, a 100-fold increase in PP1 activity and the possibility to form holoenzymes with high affinity. This chaperone-assisted PP1 expression protocol was the one used for the present work.

According to Kelker *et al.* (2009) protocol, co-transformed cells were inoculated in LB medium supplemented with kanamycin, chloramphenicol and 1mM MnCl₂ and incubated overnight at 37°C. Each 950 mL of LB were inoculated with 50 mL of started culture and supplemented with 33.3 µg/mL of kanamycin and chloramphenicol and 1mM MnCl₂. Cells were cultured at 37°C until they reached an OD₆₀₀ of 0.5. At that moment, the culture was induced with 2g/L de arabinose in order to induce the expression of GroEL/GroES chaperone. At OD₆₀₀=1, temperature was lowered to 10 °C and the overexpression of PP1 was induced with 0.1 mM de IPTG. After 20 h of expression, cells were harvested and resuspended in fresh LB supplemented with 1mM MnCl₂ and 200 µg/ml of chloramphenicol to stop ribosomal activity. For the final *in vivo* refolding step, cells were cultured at 10°C for 2 h, what increases the yield of active and well-structured PP1. Finally, cells were harvested and keep frozen at -80°C for further use.

3.2.3. Low-scale purification

After PP1 overexpression protocol, 20 ml of culture were lysed with 300 µl of lysis buffer (50mM Tris pH 8, 700 mM NaCl, 1mM MnCl₂, 10 mM Imidazole, 5% Glycerol, 0.5% Triton x-100 and 1mM PMSF) and the samples were processed as described for caspase 9 (see Material and methods 3.1.4) using Ni-NTA beads (ABT). The binding and wash buffer used for the assay was 50mM Tris pH 8, 700 mM NaCl, 1mM MnCl₂, 5% Glycerol, 10 mM Imidazole. The elution buffer was buffer B (700 mM NaCl, 50mM Tris pH 8, 1mM MnCl₂, 5% Glycerol, 250 mM Imidazole).

3.2.4. FPLC purification by affinity chromatography

Cell pellets were thawed on ice and resuspended in 50 mL of lysis buffer (50mM Tris pH 8, 700 mM NaCl, 1mM MnCl₂, 5% Glycerol, 10 mM Imidazole, 0.5% Triton x-100, half complete EDTA-free protease inhibitor cocktail tablet(Roche®)). The dissolved pellet was sonicated for 30 minutes (1 second On-1 second OFF, 30% amplitude), in a Bioblock scientific Vibra Cell 75042 sonicator. The solution was centrifuged at 17000 rpm for 30 minutes at 4°C (Sorvall RC6, SS-34 rotor). Supernatant was passed through a syringe filter of 0.45 µM diameter and it was loaded in a Nickel Affinity Cartridge 5 mL column (ABT, Agarose Beads Technologies®) using a Gilson Minipuls 3 peristaltic pump. The column was previously equilibrated with two washes, first with 5 column volumes of milliQ water and then with 5 mL column volumes of buffer A (50mM Tris pH 8, 700 mM NaCl, 1mM MnCl₂, 5% Glycerol,10 mM Imidazole). Last step was the elution of the column to obtain the desired protein using the Äkta Purifier, which was previously equilibrated with milliQ water and the used buffers. The column was initially washed with approximately 50 mL of buffer A. Then, the column was eluted with a buffer B (50mM Tris pH 8, 700 mM NaCl, 1mM MnCl₂, 5% Glycerol,250 mM Imidazole) gradient.

3.2.5. FLPC purification by size-exclusion chromatography

Once the purifying conditions for PP1 were optimized, SEC was performed using the Äkta Prime (GE Healthcare) equipment with a Superdex 75 26/60 column (Pharmacia Biotech®). The problems of instability of PP1 (it was prompt to form soluble aggregates) was solved just by adding 5% glycerol to all purification buffers. The column was equilibrated with 180 mL of SE buffer (50mM Tris pH 8, 500mM NaCl, 0.5mM TCEP, 5% glycerol) and 2.5 ml of the eluted protein from the affinity chromatography were injected into the system to perform the separation.

The fractions containing a peak in the chromatogram were run in a 10% polyacrylamide gel as described before and the fractions containing the desired protein were concentrated using a new Amicon® Ultracel 30K until the concentration was enough to perform the interaction assays.

As the protein cannot be frozen without losing its properties, this purification protocol was repeated every time an interaction assay was performed.

3.3. CHARACTERIZATION OF THE INTERACTION PP1 α - CASPASE 9

3.3.1. Pull-down assay

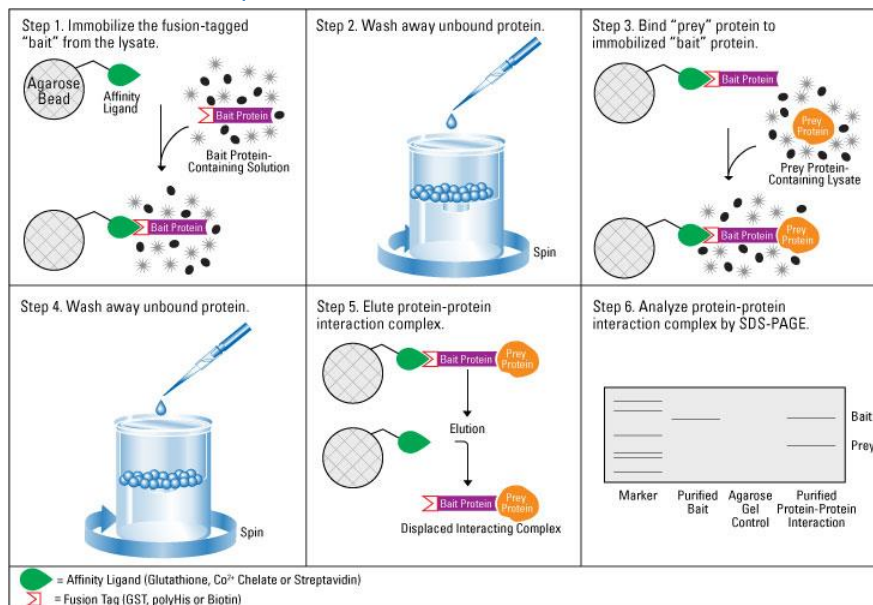


Figure 9. Pull-down assay technique. Life Technologies®, 2015

Caspase 9 and PP1 constructs were expressed according to the previously described protocol (see Material and methods 3.1.4 and 3.2.2). 20 mL of Caspase 9 and PP1 cultures were processed as described for low-scale purification protocol (see Material and methods 3.1.4 and 3.2.3). The protocol used for this assay is summarized in Figure 9. After centrifugation, aliquots of the pellet and supernatant of each construct were kept as control. The supernatant of caspase 9 constructs (CARD, Δ CARD4QC, Δ CARDC287A, C9C287AFL), as baits, was incubated for 30 minutes with the glutathione sepharose beads at 4°C. Also the supernatant of PP1_{α7-330} was incubated with the sepharose beads to perform a negative control. Then, the mixture was centrifuged for 5 minutes at

5000g (Sorvall Legend micro 21R, Thermo Scientific®). The flow-through containing the unbound proteins was separated and kept as a control. Beads were washed three times with buffer A (100 mM Tris pH 8, 200mM NaCl) to eliminate the unspecifically bound material. Then, the supernatant of Caspase 9 constructs (CARD, ΔCARD4QC, ΔCARD4C287A, C9C287AFL) was incubated for 30 minutes at 4°C. The mixture was centrifuged again and the beads were washed with buffer A. Finally, the protein-protein interaction was eluted with 100 μl of buffer B (100 mM Tris pH 8, 200mM NaCl, 20 mM Glutathion). Samples were run in a SDS-PAGE as described previously and a western blot was performed in order to confirm the presence of the two proteins in the elution.

3.3.2. Western blot analysis

A western blot analysis was performed to confirm the result of the pulldown between caspase 9 constructs and PP1_{α7-330} and PP1_{α7-300} using Nickel sepharose beads.

Protein samples previously eluted from the pull down assay were separated by SDS-PAGE at 200V for 30 minutes. Two gels were run in parallel in order to perform two western blots. They were transferred to two nitrocellulose membranes (Hybond™-ECL™) using a Trans-Blot® SD Semi-Dry Electrophoretic Transfer Cell (Biorad) at 16V during 1 hour. Then, membranes were blocked in 10 ml of blocking solution: 5% nonfat dry milk in TBST 1X (50 mM Tris HCl, pH 7.4, 150 mM NaCl, 0.1% Tween 20) for 1 h. One membrane was incubated for 1 h with Anti-His6-Peroxidase antibody (Roche). Anti-His6-Peroxidase is a monoclonal antibody for His6-tagged proteins, conjugated to horseradish peroxidase. It is able to specifically recognize the epitope of six consecutive histidine residues present in our PP1_{α7-330} recombinant protein with high sensitivity. The other membrane was incubated for 1 h with Anti-GST antibody (Anti-GST HRP Conjugate. GE Healthcare Life Sciences). Finally, membranes were washed with TBST 1X three times for 8 minutes. Protein detection was performed using 1 mL of Pierce™ ECL Western Blotting Substrate (Life Technologies). This system is based on chemiluminescent detection method. Equal volumes of two substrates, a stable peroxide solution and an enhanced luminol solution, are mixed together. When incubated with a blot on which HRP-conjugated antibodies are bound, a chemical reaction produces light that was detected by a CCD camera.

3.3.3. Biolayer Interferometry (BLI)

Biolayer Interferometry is a system to measure interactions between proteins and other biomolecules such as peptides, nucleic acids, small molecules and lipids in real time. The technique consists of the immobilization of a molecular bait on a matrix at the tip of a fiber-optic sensor. The binding between the immobilized ligand and a partner interacting molecule in an appropriate solution produces a change in optical thickness at the tip that results in a wavelength shift proportional to binding. BLI provides direct binding affinities and rates of association and dissociation. Figure 10 shows the steps of a BLI experiment.

BLI is an efficient technique to characterize molecular interaction between proteins. It only requires small amounts of protein which is a great advantage for proteins difficult to obtain.

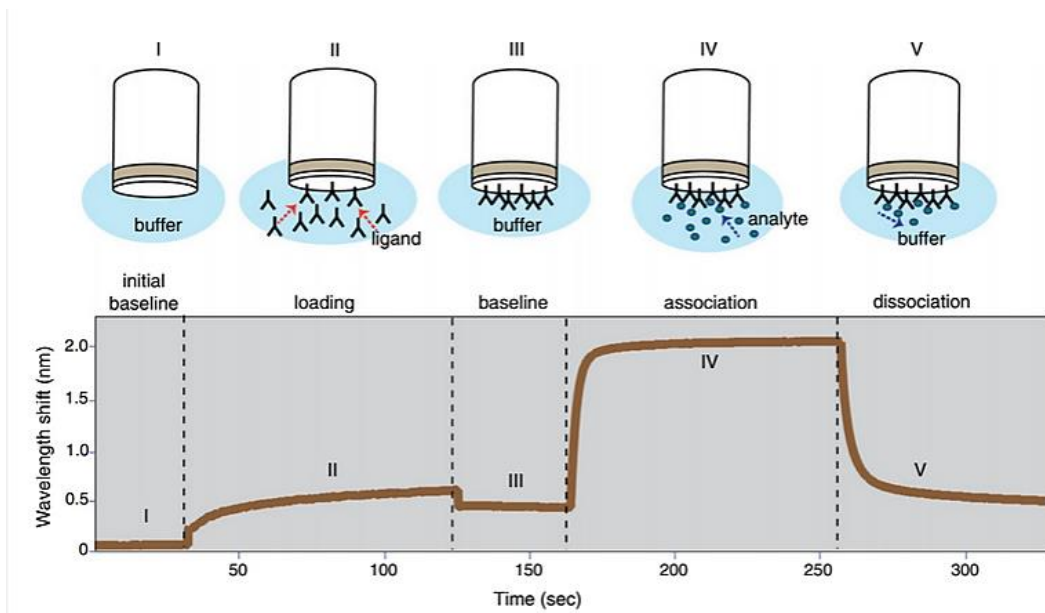


Figure 10. Experimental steps in a Biolayer Interferometry (BLI) sensogram. (I) Initial baseline using the buffer of the bait. (II) Binding of the bait protein on the BLI probe. (III) Baseline using the buffer of the prey protein. (IV) Association of the prey on the BLI probe. (V) Dissociation of the interaction (Sultana and Lee, 2015).

In the present work, the BLITz platform was used with a Ni-NTA biosensor. This biosensor is charged with novel nickel-charged-tris-nitriloacetic (Tris-NTA) groups for the capture of His-tagged molecules.

The experiment was performed immobilizing PP1, the His-tagged protein, into the sensor. PP1 was the bait protein. The prey was Caspase 9, construct C9C287AFL, containing a GST tag which does not bind to the sensor.

The protocol was performed as follows. The first step was to prepare the proteins at different concentrations (proteins were purified as described above). PP1 was diluted to 30 $\mu\text{g/ml}$ to be used as bait. The prey was prepared at different concentrations: 10mM, 5mM, 2.5mM and 1.25mM. Secondly, the biosensors were hydrated for 10 min with 250 μL of buffer (20mM Tris pH 8, 200mM NaCl, 5% glycerol, 1mM β -mercaptoethanol). Then, the steps described in Table 1. Kinetics assay steps were followed to perform the kinetic assay. The first step of the analysis was to attach the kinetic biosensor onto the BLI arm to perform the baseline measurement with buffer for 30 seconds. The second step was to pipet 4 μl of the bait protein into the drop holder and lower the arm to perform the binding of the bait to the biosensor for 180 seconds. The next step consisted of a new baseline for 1 minute. Then, 4 μl of the prey protein were placed in the drop holder to perform the binding of the protein to the partner protein immobilized onto the biosensor for 2 minutes. Finally, the dissociation step was performed by placing the arm in a new tube containing buffer.

After each experiment, the biosensors were regenerated by submerging the biosensor surface in 10mM glycine pH1.7 (5 seconds), PBS (5 seconds), 10 mM NiCl_2 to reload the biosensor (1 minute), PBS (1 minute) and 15% saccharose dissolved in PBS (5 minutes). Finally, biosensors were dried for 5 minutes at room temperature before storage.

Step	Step name	Time(s)	Step type
1	Baseline 1	30	Baseline
2	His-fusion protein	180	Loading
3	Baseline 2	60	Baseline
4	Association	120	Association
5	Dissociation	120	Dissociation

Table 1. Kinetics assay steps (Sultana and Lee, 2015)

3.3.4. Isothermal Titration Calorimetry (ITC)

Isothermal Titration calorimetry (ITC) is a very useful technique to directly study the binding energetics of protein-protein interactions, protein-ligand binding, protein-lipid binding, protein-carbohydrate binding and antigen-antibody binding. ITC can precisely determine the thermodynamic parameters associated with binding as Gibbs energy, enthalpy, entropy, binding constant and stoichiometry (Velázquez-Campoy *et al.*, 2004).

The NanoITC (TA Instruments) instrument consists of two cells placed in an adiabatic jacket connected to a computer. One cell is the reference, filled with milliQ water. The other cell is filled with a solution containing PP1. The experiment is performed at constant temperature by adding small drops of the titrant, Caspase 9, into the solution contained in the cell. The interaction between these two proteins in the system releases or absorbs heat that creates a difference of temperature in the sample cell when compared with the reference. The calorimeter calculates the parameters by measuring the amount of power required to maintain the temperature constant between the two cells. After each addition of titrant the system reaches equilibrium recording the signal as a peak. The amount of heat associated with the injection is calculated by the integration of the area under the peak and assuming the baseline as a reference (Jelesarov and Bosshard, 1999).

PP1 and Caspase9 pure proteins were diluted in the same buffer (20mM Tris pH8, 200mM NaCl, 1mM β -mercaptoethanol, 5% Glycerol), centrifuged at 14000 rpm for two minutes and degassed for 7 minutes in a degassing working station 6326 (TA Instruments®). The assay was performed at 8°C.

After several attempts with lower concentrations, 300 μ L of 20 μ M PP1 _{α 7-330} were injected in the cell and 50 μ L of his-tagged active Caspase9 full length were loaded in the buret. The titration was performed doing 30 injections of 1.5 μ L, shaking at 250rpm with 210 seconds between injections. Peak integration was performed with NanoAnalyze software.

4. RESULTS AND DISCUSSION

4.1. LOW-SCALE PURIFICATION

4.1.1. Caspase 9

Fusion protein purification using sepharose beads is the low-scale equivalent to FPLC affinity purification. In the present work, it was used to purify GST-tagged proteins and His-tagged proteins from 20 mL of cell pellets. The technique is based in four main steps: cell lysis to extract soluble proteins, protein binding, wash out of the unbound material and elution of the protein of interest.

Caspase 9 constructs were firstly overexpressed in pETGKI vector, which contains a GST purification tag. For this reason, the chosen matrix was Glutathione-sepharose beads. Samples of

pellet, supernatant and elution were taken using a buffer containing 20mM reduced glutathione that competes with the protein for the binding to the matrix. Figure 11 shows the elution of the different caspase 9 constructs.

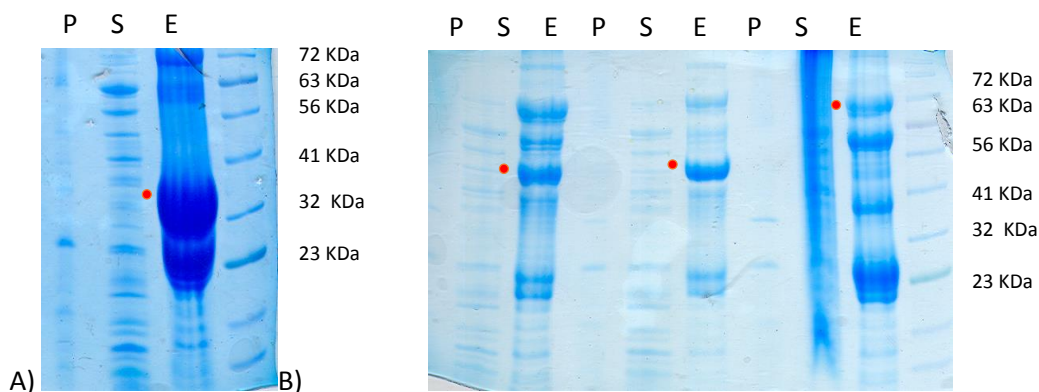


Figure 11. 10% polyacrylamide gel of the expression of CARD(A) and caspase 9 constructs Δ CARD4QC, Δ CARDC287A, FLC287A (B). Pellet (P) and supernatant (S) were used as controls. The eluted protein (E) is 38,7 KDa for CARD, 56 kDa for both Δ CARD constructs and 72KDa for full length.

CARD has a molecular weight of 12.5 KDa that together with the GST (26 KDa) appears as a band of 38 KDa. Δ CARD constructs are 30 kDa, 56 kDa with GST and C9C287A is 72 kDa. The expression amount of the three constructs seems good and there is no protein in pellet or supernatant what indicates that the protein is soluble and it was completely bound to the beads.

The expression of the mutants (Figure 12) did not yield good results. When the active site is intact, Caspase 9 appears as two processed subunits: a 62 KDa large subunit (35KDa of the catalytic subunit and 26KDa of GST tag) and a 10 KDa subunit which is not visible in the gel. The band of 26KDa corresponds to GST alone

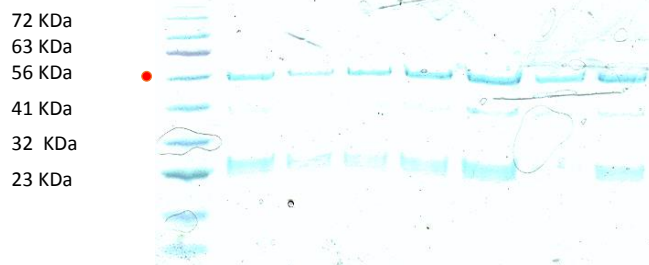


Figure 12. 10% polyacrylamide gel of the low-scale purification of T125D (lane 1 and 2) T125E (lane 3 and 4), S196D (lane 5 and 6), and C9WTFL(last lane). Mutants derived from C9WTFL in pETGKI. Caspase 9 in its wild type form is processed in a large subunit of 35 KDa +26 KDa of GST (red dot) and a small subunit of 10 KDa which is not bound to GST. The band around 26 KDa is GST alone.

It is well-known that caspase 9 is not properly overexpressed as a GST-tagged protein (Denault and Salvesen, 2002). For this reason, some problems are present. Nevertheless, the election of this tag was necessary for using the BLI assay, which requires a protein with a tag and another biomolecule (with other tag or without any tag). PP1 overexpression as a His-tagged protein is the best option to obtain stable and correctly folded protein (Peti *et al.*, 2013). This is the reason why the pETGKI vector was a good option. It is worth mentioning that the expression of caspase 9

construct in this vector was better than with other GST containing vectors tried previously in this lab.

4.1.2. PP1 α

PP1 α constructs were overexpressed in a RPB1-PP1 α vector, which contains an N-terminal Thio₆-His₆ purification tag. For this reason, the chosen matrix was Ni-NTA beads. Pellet, supernatant and Flow-through were taken as controls. The protein was eluted using a buffer containing 250mM Imidazole. As shown in Figure 13, PP1 was soluble and satisfactorily purified, eluting as a 38kDa protein (marked in red).

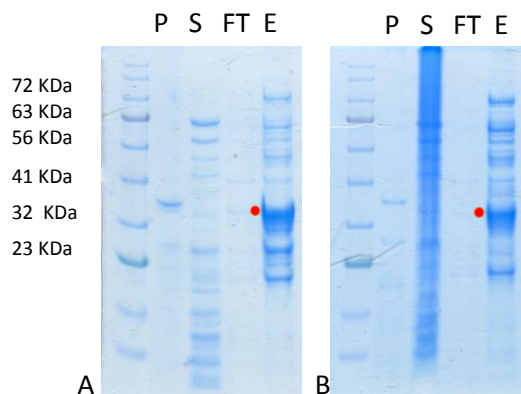


Figure 13. A).10% polyacrylamide gel of the expression of PP1 α 7-330. B) 10% polyacrylamide gel of the expression of PP1 α 7-300. Pellet (P), supernatant (S), and flow-through (FT) were used as controls. The last lane corresponds to the eluted protein (E) of 38 KDa (red dot).

4.2. CASPASE 9 FPLC PURIFICATION

4.2.1. Affinity chromatography

Caspase 9 constructs in pETGKI vector were purified using a 5 ml GST-TrapTM column as described before. The Δ CARD4QC construct did not yield any interaction with PP1 in the pull-down assay, so it was not purified for further analysis. CARD and Δ CARDC287A purification results are shown in Figure 14(A). The C9C287AFL only yield a small amount of protein that cannot be easily detected in a gel. In Figure 14(B), it is shown a concentrated fraction of the pure protein. Proteins were eluted directly with a syringe loaded with buffer B. The use of the Äkta purifier was not necessary.

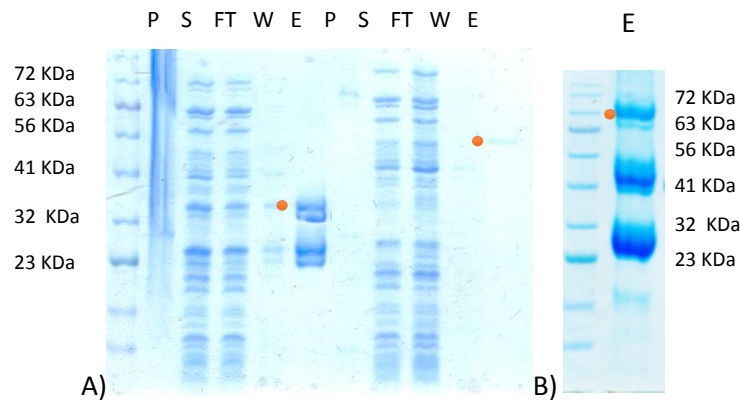


Figure 14. (A) 10% polyacrylamide gel of the affinity purification of CARD and Δ CARDC287A. Pellet (P), supernatant (S), flow-through (FT) and wash (W) were used as controls. The elution of the protein (E) corresponds to a band of 38,7 KDa for CARD construct (red dot) and 56 KDa for Δ CARDC287A (green dot). The band around 26 KDa is GST alone. (B) Concentrated fraction of the FLC287A pure protein (red dot).

The caspase 9 mutant constructs T125E and S196D expressed in pETGKI vector were purified according to the general Caspase 9 purification protocol. As shown in Figure 15, the result was not optimum due to the reasons mentioned above. The protein seems to be degraded, which is also noticeable in C9C287AFL construct purification, and there is a huge expression of GST tag alone. For this reason, the purification of mutants using this vector was not further optimized.

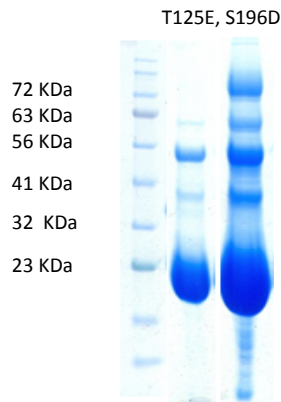


Figure 15. 10% polyacrylamide gel of the affinity purification caspase 9 mutants. From left to right T125E and S196D pure protein, respectively.

Caspase 9 wild type full length construct in pET23b vector was purified using a 5 ml Ni-NTA column as described before. Caspase 9 does not yield high amounts of pure protein but it is stable and does not degrade as it occurred to GST-tagged caspase 9 full length constructs.

In Figure 16, fractions 8 to 15 of the affinity chromatogram correspond to pure protein. The band of 35 KDa in Figure 17 is C9WTFL large subunit. The small subunit (10 KDa) can also be observed at fractions 9 and 10. The contaminant that appears at fractions 7 and 8 is Arna, an *E. coli* contaminant protein. This is not a problem because they can be nicely separated in SEC, since they have different molecular weight.

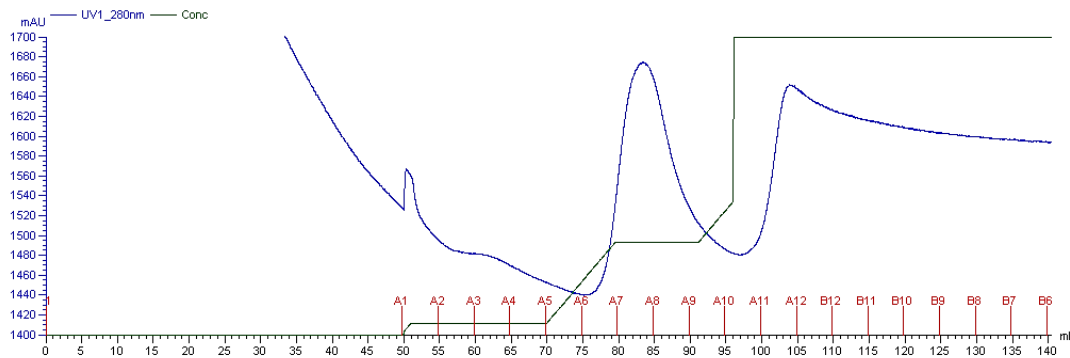


Figure 16. C9WTF1 Chromatogram of size-exclusion chromatography. The protein was eluted in 5 mL fractions. The fraction number is shown in red. The green line represents buffer B gradient. The blue line is the absorbance at 280nm.

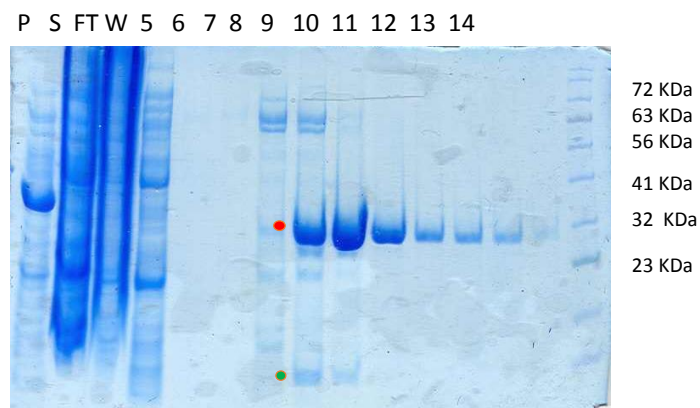


Figure 17. 10% polyacrylamide gel of the affinity purification of his-tagged caspase 9 (C9WTF1). From left to right pellet(P), supernatant(S), flow-through(FT), wash(W) and fractions 4,5,6,7,8,9,10,11,12,13,14. C9WTF1 large subunit (35 kDa) (red dot) and small subunit (10kDa) (green dot) can be observed.

4.2.2. Size-exclusion chromatography

Pure CARD caspase 9 was copurified with PP1 after 1 h of incubation at a final concentration of 200 mM NaCl. The solubility and stability of PP1 depends at a great extent of NaCl concentration. The optimum concentration is 700 mM but this high concentration disrupts the interaction between PP1 and caspase 9. For this reason, 200 mM was chosen to favor the interaction. They have almost the same molecular weight so they were difficult to separate in size-exclusion chromatography. This was performed using a Superdex 200 26/60 column. The first peak contains shown in chromatogram (Figure 18) is a protein aggregate (Figure 20). Fractions 28 to 34 contain CARD and GST alone(confirmed by western blot) and fractions 35 and 36 contain PP1 and GST alone. Finally, fractions containing pure CARD were concentrated and injected in SEC again to get pure protein.

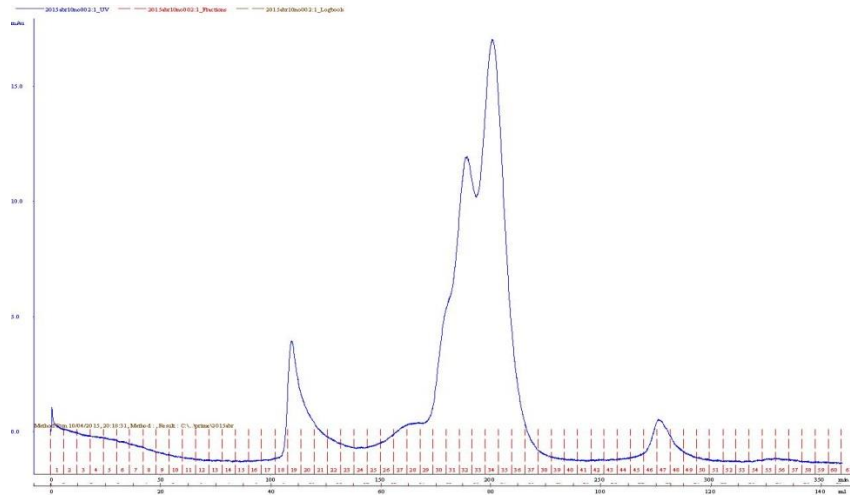


Figure 18. Chromatogram of size-exclusion chromatography of PP1+CARD. The protein was eluted in 5 mL fractions. The fraction number is shown in red. The blue line is the absorbance at 280nm.

19 20 28 29 30 31 32 33 34 35 36 46 47 48

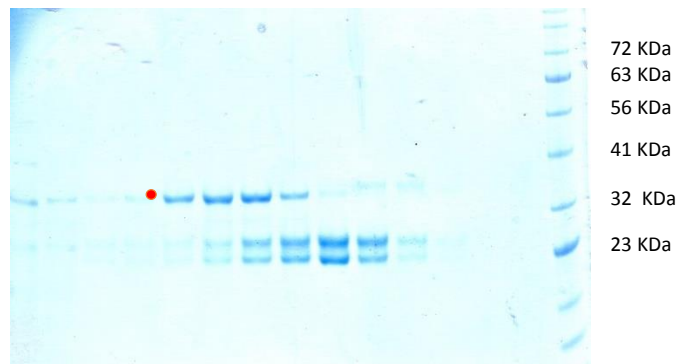


Figure 19. 10% polyacrylamide gel of the size-exclusion chromatography of CARD. CARD construct with GST has a molecular weight of 38.5 KDa (red dot). PP1 appears mixed with GST in fractions 35 and 36. The band around 26 KDa is GST alone.

Δ CARDC287A construct was copurified with PP1 also after 1h of incubation at a final concentration of 200 mM NaCl. In this case, the two proteins injected have different molecular weights. This was performed using a Superdex 200 26/60 column. Δ CARDC287A construct did not yield enough quantity of protein. So, the fractions that had a peak in the chromatogram were concentrated (Figure 20, first lane). The presence of Δ CARDC287A is confirmed but PP1 is not present in any fractions except for the input, suggesting that it was lost or degraded inside the column.

In both cases, the proteins do not elute together. This is only possible when the interaction is very strong. In this case, it is a transient interaction *in vivo* and appears to be very weak *in vitro* so this result is completely coherent since the SEC dilutes a lot the sample and any event of molecular interaction is less likely to happen.

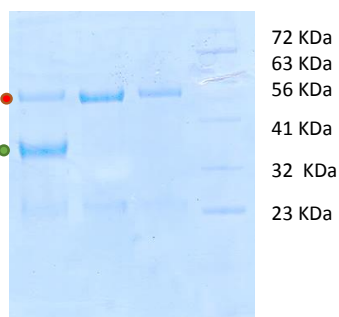


Figure 20. 10% polyacrylamide gel of the size-exclusion chromatography of Δ CARD287A and PP1. The first lane is the input (I), the fraction injected into the column containing Δ CARD287A (red dot) and PP1 (green dot). The band around 26 kDa is GST alone. The second and third lanes are 10 and 5 μ l of the concentration of fractions 25 to 30, respectively.

His-tagged C9WTF1 was injected in a Superdex 200 16/60 column as described previously. The pure protein was obtained in fractions 16 to 18 (Figure 21) that corresponds to a 35 kDa protein (Figure 22).

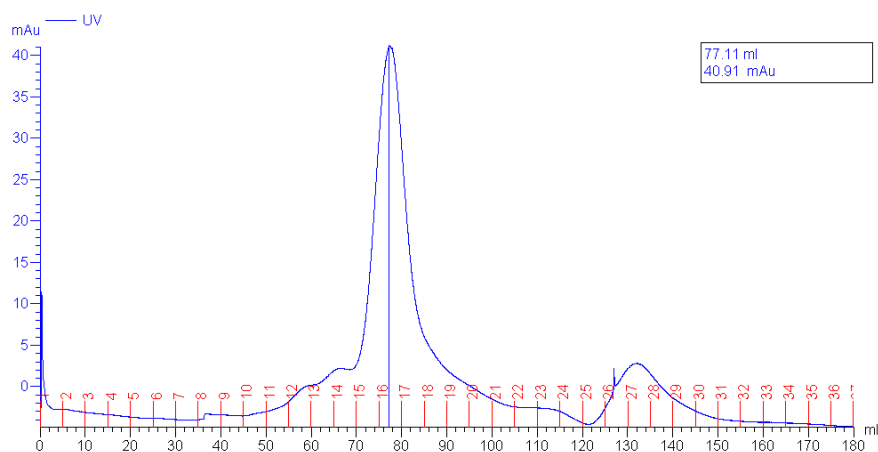


Figure 21. Chromatogram of size-exclusion chromatography of C9WTF1. The protein was eluted in 5 mL fractions. The fraction number is shown in red. The blue line is the absorbance at 280nm. Fractions 16 to 18 contain pure C9WTF1.

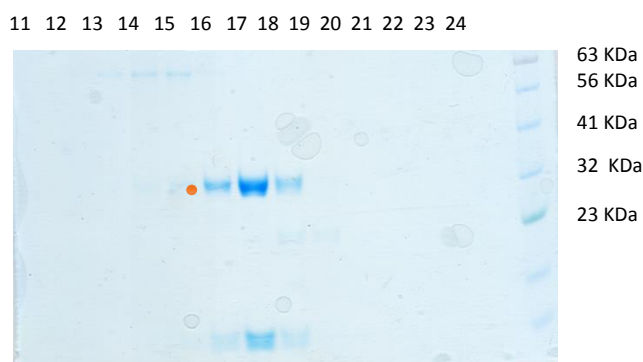


Figure 22. 10% polyacrylamide gel of the size-exclusion chromatography of C9WTF1. From left to right, fractions 11 to 24 of the chromatogram (Figure 21) The band around 35 KDa is large subunit of caspase 9 (red dot). The small subunit is also observed at 10 KDa (green dot).

4.3. PP1 α FPLC PURIFICATION

4.3.1. Affinity chromatography

PP1 is a very unstable protein. Before optimizing the conditions for PP1 purification by adding 5% glycerol to the buffers, it could not be purified alone because it formed soluble aggregates as shown in the SEC chromatogram (Figure 23). The peak corresponds to the dead volume of the column.

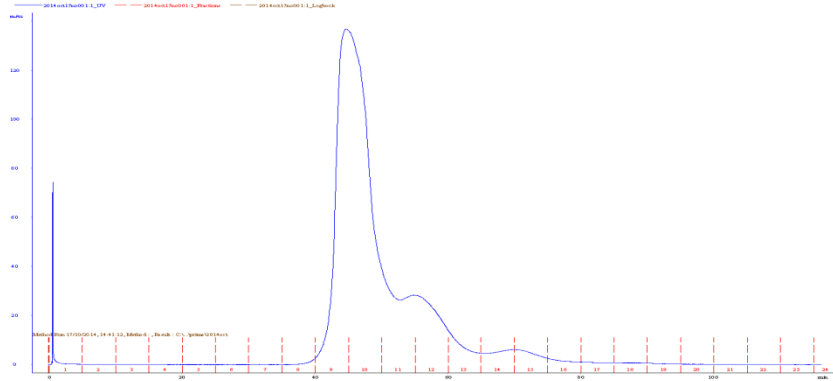


Figure 23. Chromatogram of size-exclusion chromatography of PP1. Soluble aggregates were formed before optimizing the conditions (described in Material and methods 3.2.4). The protein was eluted in 5 mL fractions. The fraction number is shown in red. The blue line is the absorbance at 280nm.

Construct PP1 _{α 7-330} was finally purified alone following the protocol described in Material and methods 3.2.4. The chromatogram in Figure 24 shows the coelution of the chaperone used in the expression protocol and PP1 at 13% of buffer B (Figure 25). After this first peak, the concentration of buffer B is set up at 100% to try to elute the rest of pure PP1. The coelution of the proteins in the affinity purification is not a problem because they are easily separated in size-exclusion chromatography since the chaperones tend to aggregate and it is eluted in the dead volume of the column.

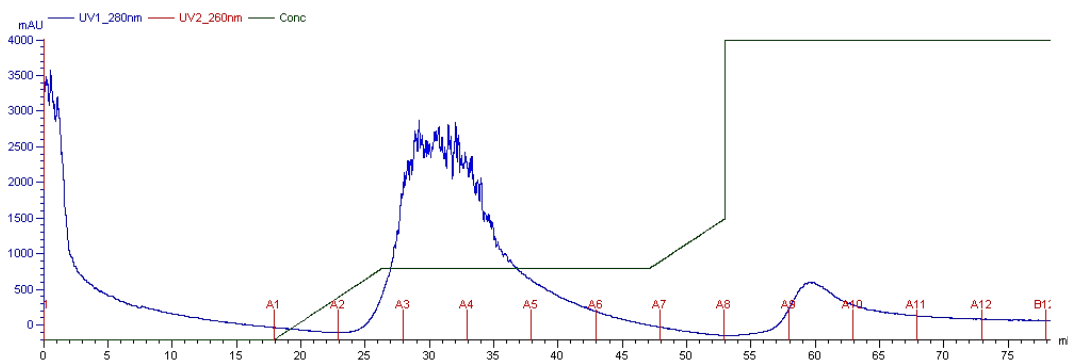


Figure 24. FPLC chromatogram of PP1 α 7-330 using a 5 mL His-Trap column. The protein was eluted in 5 mL fractions. The fraction number is shown in red. The blue line is the absorbance at 280nm. The green line indicates the percentage of buffer B used for the elution.

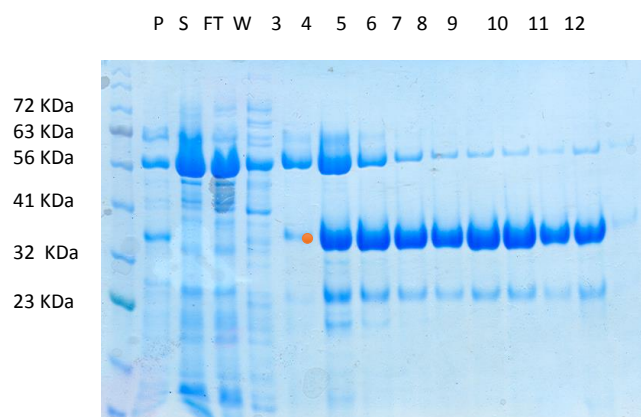


Figure 25. 10% polyacrylamide gel of the fractions of the chromatogram shown in Fig.12. From left to right: pellet(P), supernatant(S), flow-through(FT), wash(W) and fractions 3 to 12. The protein has a molecular weight of approximately 38 KDa (red dot).

The yield of the protein was good and enough to perform BLI experiments but limited for ITC. The stability of the protein diminishes rapidly with time. Even using the chaperone-assisted protocol described by Peti *et al.* (2013), the protein cannot be concentrated more than 5 μ M because it precipitates. As mentioned before, maintaining the protein concentration lower than 5 μ M it is only stable for a short period of time. For this reason, the interaction assays need to be performed immediately after purification, using fresh protein.

4.3.2. Size-exclusion chromatography

The fractions containing PP1 were concentrated and injected in a Superdex 75 16/60 column. The chromatogram (Figure 26) clearly shows two peaks, the first corresponding to an aggregate and the second to a protein of a molecular weight of approx. 40 KDa. The gel of the fractions corresponding to both peaks is shown in Figure 27. The first peak is an aggregate of the chaperones GroEL/ES which were co-expressed with PP1 α_{7-330} . The second peak, fractions 7 to 9 is pure PP1 α_{7-330} with residual degradation due to the instability of the protein.

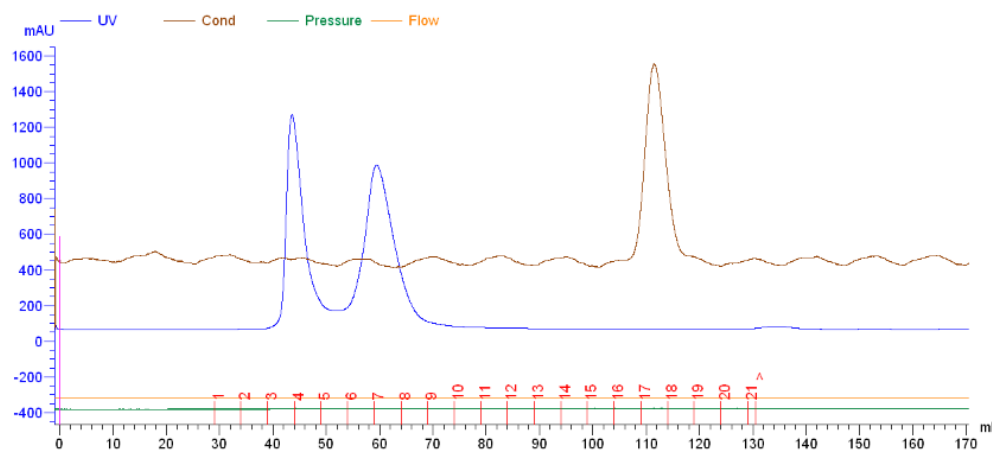


Figure 26. Chromatogram of the size-exclusion chromatography of PP1 α_{7-330} . The protein was eluted in 5 mL fractions. The fraction number is shown in red. The three first fractions correspond to the dead volume of the column. The blue line is the absorbance at 280nm.

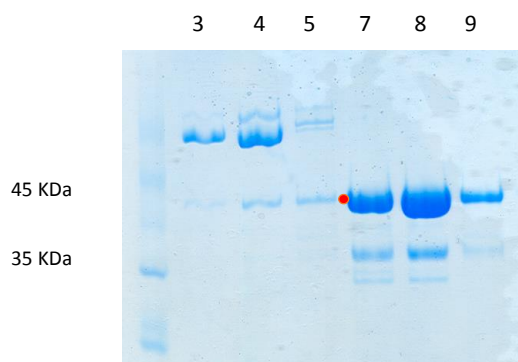


Figure 27. 10% polyacrylamide gel of the fractions of the size-exclusion chromatography (Fig.26). Fractions 3 to 5 corresponds to the aggregate of chaperones and a little amount of PP1 $_{\alpha 7-330}$. Fractions 7 to 9 contain PP1 $_{\alpha 7-330}$. The protein has a molecular weight of approximately 38 KDa (red dot).

4.4. INTERACTION STUDIES BETWEEN CASPASE 9 AND PP1 α

4.4.1. Pull-down assay between caspase 9 and PP1

The pull down assay was performed using Glutathione sepharose beads as described in Material and Methods 4.1. Caspase 9 constructs were used as bait and PP1 $_{\alpha 7-330}$ as prey. A western blot was necessary to confirm the presence of both proteins in each elution. Only the elution of each interaction was used for the western blot and a negative control proving that PP1 cannot bind to glutathione beads.

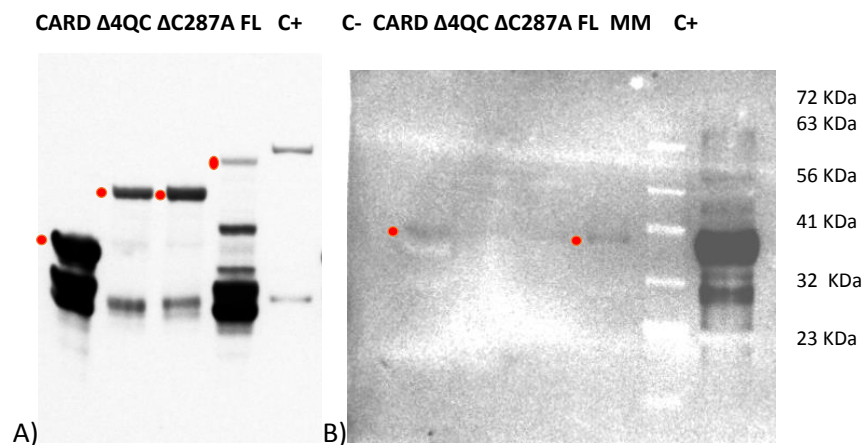


Figure 28. A) Western blot revealed with Anti-GST antibody. From left to right, the elution of PP1 $_{\alpha 7-330}$ with CARD, Δ CARD 4QC, Δ CARD C287A, C9C287AFL respectively and a positive control (a protein containing a GST tag). **B) Western blot revealed with Anti-His antibody.** From left to right, negative control, the elution of PP1 $_{\alpha 7-330}$ (red dot) with CARD, Δ CARD 4QC, Δ CARD C287A, C9C287AFL respectively; molecular marker and a positive control.

Figure 28A shows the detection of caspase 9 constructs in each elution using Anti-GST antibody directly conjugated with horseradish peroxidase (HRP). Figure 28B shows the detection of PP1 in the same elution using an anti-His antibody conjugated also with HRP. The aim was to perform a qualitative western blot, to detect absence or presence of the protein to prove the *in vitro* interaction. PP1 $_{\alpha 7-330}$ was clearly detected in CARD and C9C287AFL constructs. The best PP1 signal is for the elution with C9C287AFL although this caspase has the lowest signal in Figure 28A. This

suggests that the interaction is even stronger and caspase 9 is required as full length for the *in vitro* interaction with PP1. On the other hand, the signal is very weak for Δ CARD 4QC and Δ CARDC287A, especially for the former. It is worth mentioning that the mutations in Δ CARD 4QC were selected to force the dimerization of caspase 9 for crystallization studies. Therefore, this may diminish the capacity of the protein to interact with PP1.

However, this western blot was performed only as a first approach. The assay is qualitative, so the conclusions are limited but it was useful for further interaction assays.

In another experiment, the same protocol previously described was followed using pure protein instead of *E. coli* culture lysates. Protein concentration was measured by spectrophotometry to perform the assay with equimolar concentration of both proteins.

The caspase 9 constructs CARD, Δ CARDC287A and C9C287AFL were chosen for the assay in order to validate the preliminary results obtained in the previous pull-down experiment.

The elution of Δ CARDC287A and PP1 did not provide a positive result. Only Δ CARDC287A was retained in glutathione sepharose beads. The interaction was not strong enough to anchor PP1, which was lost in flow-through (data not shown).

Also, a pulldown was performed with pure CARD and PP1 in order to determine if CARD domain was enough to maintain the interaction. The result was negative (data not shown). The CARD protein aliquot used was kept at -80 °C prior to use. According to our experience this is not an ideal situation for caspases and may disturb the stability of the protein, being the cause of the negative result.

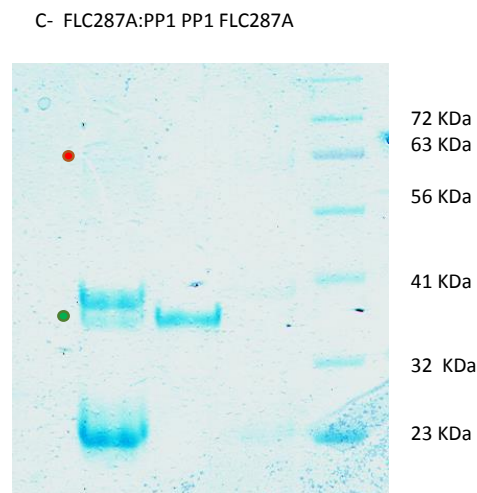


Figure 29. 10% polyacrylamide gel of the pull-down assay using GST beads , pure PP1 as prey and pure C9C287AFL as bait. From left to right, negative control, C9C287A:PP1 elution, pure PP1 and pure C9C287AFL. PP1 is clearly present in the elution (green dot) and C9C287A (red dot) appears as a band of 72 KDa lightly visible.

In contrast, the interaction between C9C287AFL and PP1 was detected. As shown in Figure 29, both PP1 and caspase 9 coelute. The first lane is a negative control to demonstrate that PP1 cannot

interact with glutathione sepharose beads. This proves that the presence of PP1 in the elution (second lane) is due to specific interaction with caspase 9. The third and fourth lanes contain pure PP1 and C9C287AFL, respectively. The band pattern of the elution is a mixture between the band pattern of caspase 9 alone and pure PP1.

4.4.2. Biolayer Interferometry (BLI)

The experiment was performed as described in Material and methods 4.1. Figure 30 shows the kinetics assay between PP1 as bait and C9C287AFL construct as prey. The assay was done three different times with similar results. The resulting dissociation constant was near 3.8×10^{-7} . However, some unspecific binding of caspase 9 to the sensor was observed. Conditions need to be optimized to adjust the resulting K_d .

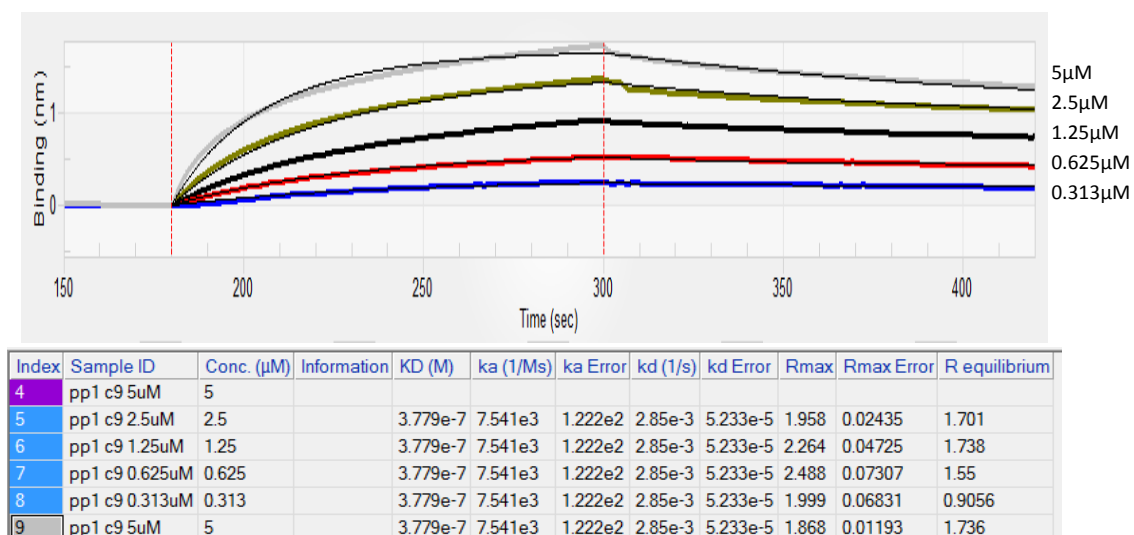


Figure 30. Kinetic assay using Ni-NTA sensors. His-tagged PP1 is the bait at $20 \mu\text{M}$ and construct C9C287AFL is the prey at 5 (grey), 2.5 (green), 1.25 (black), 0.625 (red), 0.313 (blue) μM .

The kinetic assay between CARD and PP1 cannot be performed properly because there was too much unspecific binding of caspase 9 to the Ni-NTA sensor. The experimental conditions need to be optimized.

Figure 31 shows the kinetics assay between PP1 as bait and $\Delta\text{CARD}287\text{A}$ construct as prey. The resulting dissociation constant is under the detection limit of the equipment. For this reason, the experiment was not further optimized.

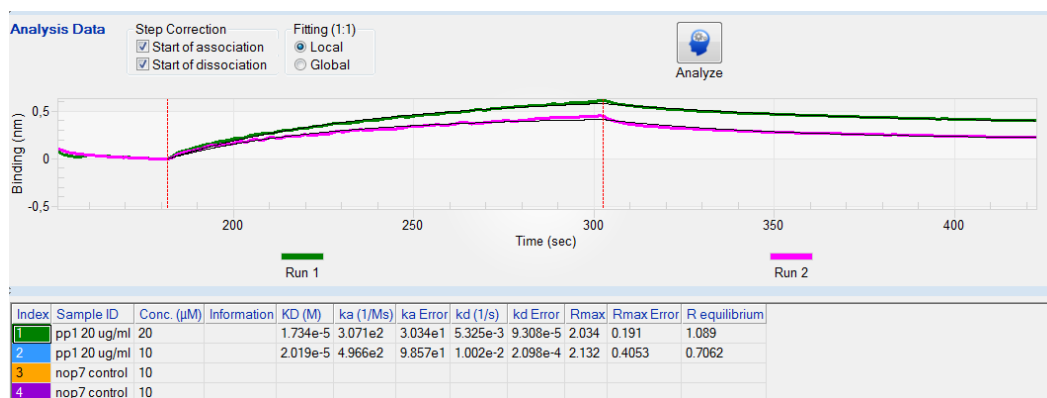


Figure 31. Kinetic assay using Ni-NTA sensors. His-tagged PP1 is the bait at 20 μM and construct ΔCARD287A is the prey at 20 (green) and 10 (pink) μM.

These experiments lead to several conclusions. Although the kinetic assay needs to be optimized to avoid residual unspecific binding, the results show that the interaction between C9C287AFL and PP1 is much stronger than the interaction between ΔCARD287A and PP1, which is under the detection limit of the technique. This evidence is consistent with the results mentioned in 4.4.1 and 4.4.2 and support the idea that caspase 9 needs both CARD and ΔCARD domain to form a significant *in vitro* interaction with PP1. This is also consistent with the results obtained by Dessauge *et al* (2006) as they determined two main binding sites in caspase 9 for the interaction with PP1: one located in CARD domain and the other in the catalytic domain.

In a previous review, Bollen (2001) proposed a combinatorial control of PP1 in which the binding of PIPs to the phosphatase is mediated by multiple, degenerated short sequence motifs functioning as interacting sites (Figure 32). The primary PP1-binding motif in PIPs is the RVxF motif, and it is accepted that it functions as an anchor for PP1 and allows its partner protein to make additional interactions with the phosphatase. These additional contacts can be weak but the multiple binding sites ensure a tight interaction. PIPs differ in the number and type of the PP1-docking sites and as they are degenerated, some sequence variants considerably affect the affinity for PP1. Hence, the disruption of only a single motif can be enough to weaken (Beullens *et al*.2000) or even break the interaction (Aggen *et al*, 2000 and Liu *et al*, 2000). Then, it is likely that neither CARD nor ΔCARD are enough to maintain the *in vitro* binding and both domains are required to establish an efficient interaction.

This may have an important biological significance and it is consistent with the molecular mechanism of caspase 9 in the context of apoptosis. If PP1 only binds to the whole caspase 9, this means that the dephosphorylation and consequent activation occurs before caspase 9 is processed in the apoptosome. Thus, the kinase/phosphatase crosstalk is a control point before caspase 9 is processed as a mature protein and its protease activity becomes activated.

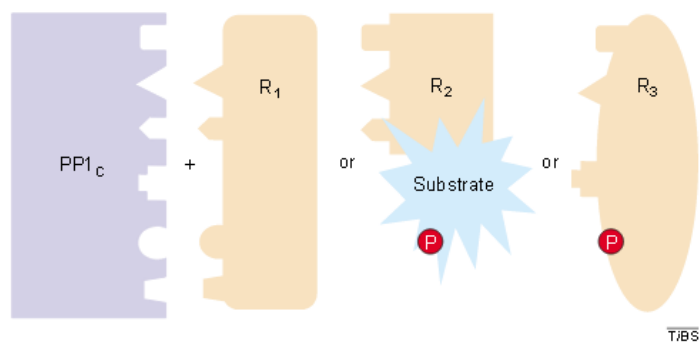


Figure 32. Combinatorial-control model of the catalytic subunit of protein phosphatase 1 (PP1_c) proposed by Bollen (2001). The catalytic subunit is represented with six different binding sites for the regulatory (R) subunits. The R subunits act as activity-modulators (R1), targeting proteins (R2) and/or substrates (R3). Caspase 9 would be a R3-type subunit. It is suggested that the R subunits have multiple contacts with PP1_c and that they can share binding sites. Specificity is achieved by interaction with specific subsets of binding pockets on PP1_c.

Another conclusion is that the *in vitro* interaction between these two proteins is weak. This was expected because these proteins form transient interactions in the cell that are crucial for signaling transduction in apoptosis. Also, they are regulated by protein reversible phosphorylation which may have an important role in the increase of the affinity between these two proteins, as it is discussed below.

4.4.3. Isothermal Titration Calorimetry (ITC)

The *in vitro* interaction between PP1_{α7-330} and caspase 9 full length was also studied by ITC experiments. After several attempts with lower concentrations, 300μL of 20μM PP1_{α7-330} were injected in the cell and 50μL of his-tagged active C9WTFL were loaded in the buret. The titration was performed doing 30 injections of 1,5μL, shaking at 250rpm with 210 seconds between injections. Peak integration was performed with NanoAnalyze software.

The results are shown in Figure 33 and suggest that there is a weak interaction between the proteins but as caspase 9 concentration is lower than necessary to perform an optimized interaction ITC assay, the software is not able to do a good adjustment of the model and precisely determine the kinetic parameters. The purification of C9WTFL did not yield enough quantity of protein to perform different experimental conditions. Hence the conclusions derived from these preliminary results are limited. It would be interesting to repeat the experiment using higher concentrations of caspase 9. This way, the equipment would register better signal and the adjustment of the kinetic parameters would be much more accurate.

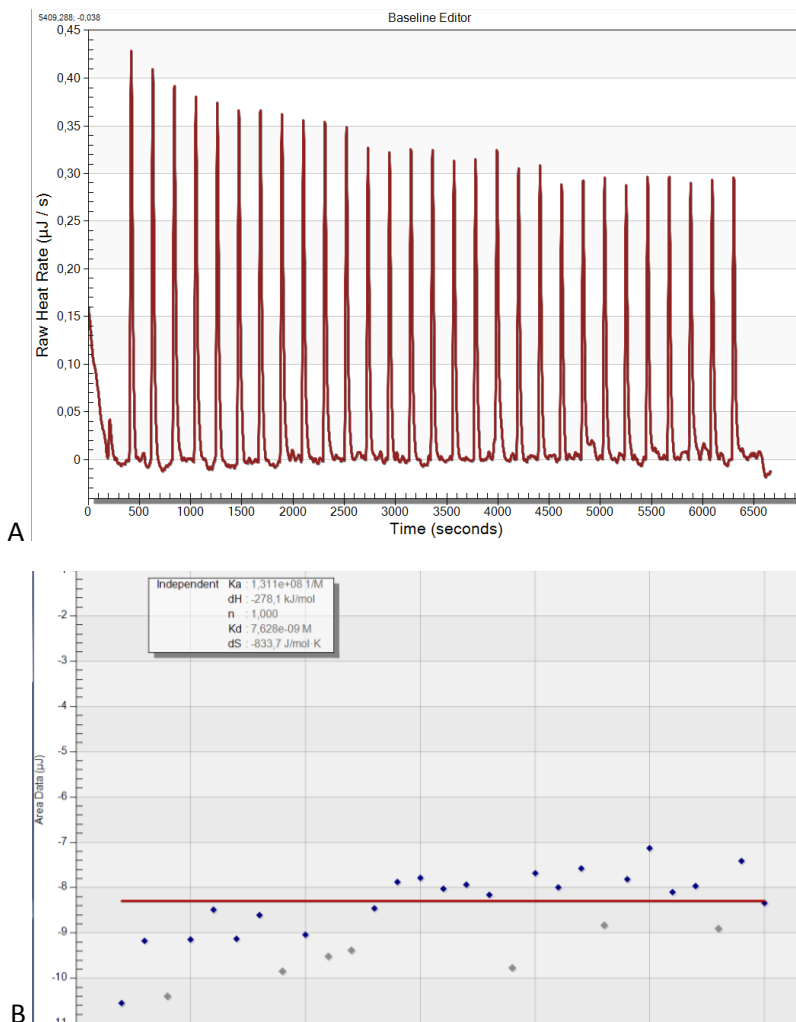


Figure 33. ITC for PP1 and C9WTF1. A) The graph represents the values of heat released ratio ($\mu\text{J/s}$) versus time (s). The titration was performed doing 30 injections of $1.5\mu\text{L}$, shaking at 250rpm with 210 seconds between injections. The temperature of the cell was 8°C . B) Adjustment of the kinetic model. The fitting of the experimental points is deficient. More concentration of C9WTF1 would be necessary in order to perform an accurate adjustment of the model and provide kinetic parameters.

It is very important to take into account that this interaction *in vivo* occur under certain stimuli and work under complicated regulatory mechanisms in which hundreds of proteins are involved. It is possible that these two proteins, as it is usually the case for PP1, need regulatory additional proteins to control their binding or additional post-translational modifications that are not present in our recombinant proteins. The phosphorylation event might be crucial in the recognition of caspase 9 by the phosphatase and also it might increase the affinity of the interaction. Caspase 9 has no described PP1-binding motifs other than RVxF. SILK or MyPhoNe motifs are not present N-terminal to RVxF so it is likely that the affinity of the interaction relies entirely in the RVxF motifs present and other caspase 9 specific motifs not yet described.

Next step would be to perform the same experiments using the phosphomimetics mutants designed in the present work to study whether the affinity of the interaction is affected. These

candidates have been selected as PP1 targets for several reasons. All of them have known kinases that phosphorylate them in the context of the apoptosis pathway.

Parrish *et al* (2013) highlighted Thr 125 as an important target residue for post-translational modifications since it is conserved among evolution and it is regulated by different signaling pathways. ERK kinase, the cycling dependent kinase (CDK1), DYRK1A and p38 α can phosphorylate this residue, decreasing caspase 9 activation and its proteolytic activity. But there is no known phosphatase targeting this threonine situated in the linker between CARD and the catalytic domain of caspase 9.

Furthermore, S196 is another potential target for PP1, as it is surrounded by a RVxF motif (Figure 35). Bollen (2001) reviewed that for some PP1-binding partners a phosphorylation event near or within a RVxF motif strengthens their interaction with PP1. This residue is also an Akt target (Cardone *et al.* 1998), an anti-apoptotic kinase that inactivates by phosphorylation of pro-apoptotic factors such as Bad or pro-caspase 9, which are also PP1 target proteins. Most importantly, this residue is located inside the Δ CARD binding region described by Dessauge *et al.* (2006). Moreover, Akt is negatively regulated upstream of the apoptotic pathway by PP1. This suggests the hypothesis that Ser 196 residue of caspase 9 might be dephosphorylated by PP1, completing a perfect interplay between the anti-apoptotic kinase and the pro-apoptotic phosphatases in the regulation of caspase 9 activation (Figure 34).

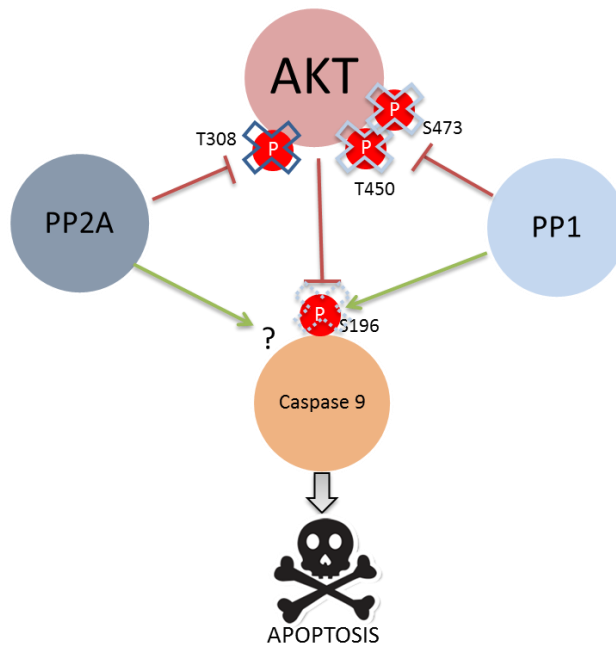


Figure 34. Schematic representation of the interplay between the kinase AKT, phosphatases PP1 and PP2A and caspase 9, the last initiator caspase in the apoptotic pathway. AKT is a kinase that directly phosphorylates caspase 9 by targeting Ser 196 residue. As a result, the proteolytic activity of caspase 9 is significantly reduced, preventing further pro-apoptotic signaling. On the other hand, two proteins inactivate AKT by dephosphorylating particular residues: T450 and S473 are targets of PP1 and T308 of PP2A. It is also known that both phosphatases directly interact with caspase 9 but their dephosphorylation target residues remain unknown. Since caspase 9 has a PP1 RVxF binding motif surrounding S196 and PP1 acts as an inhibitor of AKT action, we hypothesize that this phosphatase might be responsible for S196 dephosphorylation, antagonizing AKT anti-apoptotic signaling.



Figure 35. Caspase 9 sequence fragment. S196 is phosphorylated by Akt (Cardone et al., 1998) because it recognizes a motif surrounding this residue (blue rectangle). Also, caspase 9 sequence has a PP1-binding RVxF motif surrounding S196 (orange rectangle). This motif usually has N-terminal basic residues (highlighted in green) and C-terminal acidic residues (shown in red). As it fulfills the requirements, we hypothesized that S196 could be the dephosphorylated caspase 9 residue by PP1.

Further experiments with caspase 9 phosphomimicking mutants will be performed to elucidate the candidate residue to be phosphorylated by PP1, shedding light in the activation of Caspase 9 in the apoptotic pathway.

The structural knowledge about PP1 motifs and interactions can be used to design therapeutical approaches. As described in literature for the same family member PP2A (Arrous et al, 2013), small molecule compounds such as peptides can compete with specific binding motifs and disrupt the interaction between PP1 and its PIPs.

5. CONCLUSIONS

- The interaction between caspase 9 and PP1 is weak, as expected for transient interactions.
- The interaction is only detectable using caspase 9 full length construct. Neither CARD nor ΔCARD domains are enough to maintain *in vitro* binding, as both domains are required to establish an efficient interaction. This confirms that *in vivo* dephosphorylation and consequent activation occurs before caspase 9 is processed in the apoptosome.
- The phosphorylation event might be crucial in the recognition of caspase 9 by the phosphatase and also it might increase the affinity of the interaction. Recombinant proteins from heterologous expression in *E. coli* didn't show high affinity probably because of the lack of posttranslational modifications.
- According to the literature, phosphomimetic caspase 9 mutants were designed as potential PP1 phosphorylation site candidates. In further experiments, the affinity between these caspase 9 mutants will be evaluated.

6. BIBLIOGRAPHY

- AGGEN, JB.; NAIRN, AC.;CHAMBERLIN, R. (2000). Regulation of phosphatase-1. *Chem Biol*, 7(1):R13-23.
- AGILENT TECHNOLOGIES®, 2015. *QuikChange II Site-Directed Mutagenesis Kits - Details & Specifications*. Visited on 24th June, 2015
<http://www.genomics.agilent.com/article.jsp?pagelId=384>
- AYLLON, V.; MARTÍNEZ, A.; GARCÍA, A.; CAYLA, X.; REBOLLO, A. (2000) Protein phosphatase 1 α is a Ras-activated Bad phosphatase that regulates interleukin-2 deprivation-induced apoptosis. *EMBO*, 19(10): 2237–2246.
- BEULLENS, M.; VULSTEKE, V.; VAN EYNDE, A.; JAGIELLO, I.; STALMANS, W.; BOLLEN, M. (2000). The C-terminus of NIPP1 (nuclear inhibitor of protein phosphatase-1) contains a novel binding site for protein phosphatase-1 that is controlled by tyrosine phosphorylation and RNA binding. *Biochemical Journal*, 352:651–658.
- BOLLEN, M. (2001). Combinatorial control of protein phosphatase-1. *Trends in Biochemical Science*, 26(7):426-31.
- BOLLEN, M.; PETI, W.; RAGUSA, MJ.; BEULLENS, M. (2010). The extended PP1 toolkit: designed to create specificity. *Trends in Biochemical Science*, 35(8):450-458
- BONSOR, D.; BUTZ, S.F.; SOLOMONS, J.; GRANT, S.; FAIRLAMB, I.J.S.; FOGG, M.J.; GROGAN, G. (2006). Ligation independent cloning (LIC) as a rapid route to families of recombinant biocatalysts from sequenced prokaryotic genomes. *Org. Biomol. Chem.*, 4: 1252-1260.
- CARDONE, MH.; ROY, N.; STENNICKE, HR.; SALVESEN GS.; FRANKE, TF.; STANBRIDGE, E.;FRISCH, S.; REED, JC. (1998). Regulation of cell death protease caspase-9 by phosphorylation. *Science*, 282(5392):1318-21.
- DENAULT, JB.; SALVESEN, GS. (2001) Caspases. *Current protocols in protein science*, 21.8.1-21.8.16
- DENAULT, JB.; SALVESEN, GS. (2002). Expression, purification and characterization of caspases. *Current protocols in protein science*, 21.13
- DESSAUGE, F.;CAYLA, X;ALBAR, JP.;FLEISHCHER, A.;GHADIRI, A.;DUHAMEL, M., REBOLLO, A. (2006). Identification of PP1 α as a Caspase-9 regulator in IL-2 deprivation-induced apoptosis. *J Immunol*, 177;2441-2451.
- DOHONEY, KM.; GUILLERM, C.; WHITEFORD, C.; ELBI, C.; LAMBERT, PF.; HAGER, GL.; BRADY, JN. (2004) Phosphorylation of p53 at serine 37 is important for transcriptional activity and regulation in response to DNA damage. *Oncogene*, 23: 49–57.
- FIGUEREIDO, J; DA CRUZ E SILVA, O; FARDILHA, M. (2014). Protein Phosphatase 1 and its complexes in carcinogenesis. *Current Cancer Drug Targets*, 14,2-29.
- HASSAN, M.; WATARI,H.;ABUALMAATY, A.; OHBA, Y.; SAKURAGI, N. (2014) Apoptosis and molecular targeting therapy in cancer. *Biomed Research International*, 2014:150845
- JELESAROV, I.; BOSSHARD, H.R. (1999). Isothermal titration calorimetry and differential scanning calorimetry as complementary tools to investigate the energetics of biomolecular recognition. *Journal of Molecular Recognition*.12:3-18
- KANG, JS.; KIM, SH.; HWANG, MS.; LEE, YC.;KIM, YJ. (2001) The structural and functional organization of the yeast mediator complex. *J Biol Chem*, 276(45):42003-10

- KELKER, MS.; PAGE, R.; PETI, W. (2009) Crystal structures of protein phosphatase-1 bound to nodularin-R and tautomycin: a novel scaffold for structure based drug design of serine/threonine phosphatase inhibitors. *J Mol Biol*, 385(1): 11–21.
- KUO, Y. C.; HUANG, K. Y.; YANG, C. H.; YANG, Y. S.; LEE, W. Y.; CHIANG, C. W. (2008) Regulation of phosphorylation of Thr-308 of Akt, cell proliferation, and survival by the B55 α regulatory subunit targeting of the protein phosphatase 2A holoenzyme to Akt. *J. Biol. Chem*, 283, 1882-1892.
- LIFE TECHNOLOGIES [®], 2015. *Pull-down assay*. Visited on 20th June, 2015 <https://www.lifetechnologies.com/es/en/home/life-science/protein-biology/protein-biology-learning-center/protein-biology-resource-library/pierce-protein-methods/pull-down-assays.html>
- LI M.; STEFANSSON B.; WANG W.; SCHAEFER E.M.; BRAUTIGAN D.L. (2006). Phosphorylation of the Pro-X-Thr-Pro site in phosphatase inhibitor-2 by cyclin-dependent protein kinase during M-phase of the cell cycle. *Cell. Signal*, 18:1318–1326.
- LIU, J.;BRAUTIGAN, DL. (2000) Glycogen synthase association with the striated muscle glycogen-targeting subunit of protein phosphatase-1. Synthase activation involves scaffolding regulated by β -adrenergic signalling. *J. Biol. Chem*. 275, 26074–26081
- LÓPEZ-OTÍN, C.; HUNTER, T. (2010). The regulatory crosstalk between kinases and proteases in cancer. *Nat Rev Cancer.*, (4):278-92.
- PARRISH, AB.; FREEL, CD.; KORNBLUTH, S. (2013) Cellular mechanisms controlling caspase activation and function. *Cold Spring Harb Perspect Biol*, 5:a008672
- PETI, W.; NAIRN, AC.; PAGE, R. (2013) Structural basis for protein phosphatase 1 regulation and specificity. *FEBS*, 280(2): 596–611.
- PETI, W.; PAGE, R. (2007) Strategies to maximize heterologous expression in *Escherichia coli* with minimal cost. *Protein Expr Purif*, 51(1):1-10.
- QIN, H.; SRINIVASULA, SM.; WU, G.; FERNANDES-ALNEMRI, T.; ALNEMRI, E.S.; SHI, Y. (1999) Structural basis of procaspase-9 recruitment by the apoptotic protease-activating factor 1. *Nature*, 399(6736):549-57.
- RENATUS, M.; STENNICKE, HR.; SCOTT, FL.; LIDDINGTON, RC.; SALVESEN, GS. (2001). Dimer formation drives the activation of the cell death protease caspase 9. *PNAS* 98(25):14250-5.
- SINGH TD.; BASHAM ME.; NORDEEN EJ.; NORDEEN KW. (2000). Early sensory and hormonal experience modulates age-related changes in NR2B mRNA within a forebrain region controlling avian vocal learning. *J Neurobiol*, 44:82–94.
- SRINIVASULA, SM.; AHMAD, M.; FERNANDES-ALNEMRI T.; ALNEMRI, ES. (1998) Autoactivation of procaspase-9 by Apaf-1- mediated oligomerization. *Molecular Cell*, 1(7):949-57.
- SULTANA, A.; LEE, JE. (2015). Measuring protein-protein and protein-nucleic acid interactions by biolayer interferometry. *Curr. Protoc. Protein Sci*. 79:19.25.1-19.25.26.
- TAYLOR, RC.; CULLEN, SP.; MARTIN, SJ. (2007) Apoptosis: controlled demolition at the cellular level. *Nat Rev Mol Cell Biol*, 9(3):231-41.
- VAN HOOFF, C.; GORIS, J. (2003) Phosphatases in apoptosis: to be or not to be, PP2A is in the heart of the question. *Biochim Biophys Acta*, 1640:97–104.
- VELÁZQUEZ-CAMPOY, A.; OHTAKA, H.; NEZAMI, A.; MUZAMMIL, S.; FREIRE, E. (2004) Isothermal titration calorimetry, in: *Current protocols in Cell Biology*. John Wiley and sons. Inc. 17.8.1-17.8.24

- XIAO, L.; GONG, L-L.; YUAN, D.; DENG, M.; ZENG, X-M.; CHEN, L-L.; ZHANG, L.; YAN, Q.; LIU, X-H.; SUN, S-M.; LIU, J.; MA, H-L.; ZHENG, C-B.; FU, H.; CHEN, P-C.; ZHAO, J-Q.; XIE, S-S.; ZOU L-J.; XIAO, Y-M; LIU, W-B.; ZHANG, J.; LIU, Y.; LI, DW-C. (2010) Protein phosphatase-1 regulates Akt1 signal transduction pathway to control gene expression, cell survival and differentiation. *Cell Death and Differentiation*, 17,1448-1462
- WEINBERG, R. (2007) *Molecular Biology of Cancer*. 2nd Edition. Ed. Garland Science